



OPEN ACCESS

Edited by:

Claudia Torino,
Italian National Research Council, Italy

Reviewed by:

Tiziano Verri,
University of Salento, Italy
Eleanor DeLand Lederer,
University of Texas Southwestern
Medical Center, United States

***Correspondence:**

Silvia Dossena
silvia.dossena@pmu.ac.at
Tamás Nagy
nagy.tamas@pte.hu

† Present address:

Roberta Costa,
Aptuit Srl, Verona, Italy
Alessia Remigante,
Institute of Biophysics, National
Research Council, Genoa, Italy

‡ These authors have contributed
equally to this work

Specialty section:

This article was submitted to
Molecular Medicine,
a section of the journal
Frontiers in Cell and Developmental
Biology

Received: 16 September 2020

Accepted: 23 October 2020

Published: 19 November 2020

Citation:

Costa R, Remigante A, Civello DA,
Bernardinelli E, Szabó Z, Morabito R,
Marino A, Sarikas A, Patsch W,
Paulmichl M, Janáky T, Miseta A,
Nagy T and Dossena S (2020)
O-GlcNAcylation Suppresses the Ion
Current IC_{ISwell} by Preventing the
Binding of the Protein IC_{IN} to
 α -Integrin.
Front. Cell Dev. Biol. 8:607080.
doi: 10.3389/fcell.2020.607080

O-GlcNAcylation Suppresses the Ion Current IC_{ISwell} by Preventing the Binding of the Protein IC_{IN} to α -Integrin

Roberta Costa^{1†‡}, Alessia Remigante^{1,2†‡}, Davide A. Civello¹, Emanuele Bernardinelli¹, Zoltán Szabó³, Rossana Morabito², Angela Marino², Antonio Sarikas¹, Wolfgang Patsch¹, Markus Paulmichl⁴, Tamás Janáky³, Attila Miseta⁵, Tamás Nagy^{5*} and Silvia Dossena^{1*}

¹ Institute of Pharmacology and Toxicology, Paracelsus Medical University, Salzburg, Austria, ² Department of Chemical, Biological, Pharmaceutical and Environmental Sciences, University of Messina, Messina, Italy, ³ Department of Medical Chemistry, Faculty of Medicine, University of Szeged, Szeged, Hungary, ⁴ Department of Personalized Medicine, Humanomed, Klagenfurt, Austria, ⁵ Department of Laboratory Medicine, Medical School, University of Pécs, Pécs, Hungary

O-GlcNAcylation is a post-translational modification of proteins that controls a variety of cellular processes, is chronically elevated in diabetes mellitus, and may contribute to the progression of diabetic complications, including diabetic nephropathy. Our previous work showed that increases in the O-GlcNAcylation of cellular proteins impair the homeostatic reaction of the regulatory volume decrease (RVD) after cell swelling by an unknown mechanism. The activation of the swelling-induced chloride current IC_{ISwell} is a key step in RVD, and IC_{IN}, a ubiquitous protein involved in the activation of IC_{ISwell}, is O-GlcNAcyated. Here, we show that experimentally increased O-GlcNAcylation of cellular proteins inhibited the endogenous as well as the IC_{IN}-induced IC_{ISwell} current and prevented RVD in a human renal cell line, while decreases in O-GlcNAcylation augmented the current magnitude. In parallel, increases or decreases in O-GlcNAcylation, respectively, weakened or stabilized the binding of IC_{IN} to the intracellular domain of α -integrin, a process that is essential for the activation of IC_{ISwell}. Mutation of the putative YinOYang site at Ser67 rendered the IC_{IN}-induced IC_{ISwell} current unresponsive to O-GlcNAc variations, and the IC_{IN} interaction with α -integrin insensitive to O-GlcNAcylation. In addition, exposure of cells to a hypotonic solution reduced the O-GlcNAcylation of cellular proteins. Together, these findings show that O-GlcNAcylation affects RVD by influencing IC_{ISwell} and further indicate that hypotonicity may activate IC_{ISwell} by reducing the O-GlcNAcylation of IC_{IN} at Ser67, therefore permitting its binding to α -integrin. We propose that disturbances in the regulation of cellular volume may contribute to disease in settings of chronically elevated O-GlcNAcylation, including diabetic nephropathy.

Keywords: O-GlcNAcylation, IC_{ISwell}, IC_{IN}, α -integrin, regulatory volume decrease, kidney, protein-protein interaction

INTRODUCTION

O-GlcNAcylation is a dynamic and abundant post-translational modification of cytosolic, nuclear, mitochondrial, and membrane proteins, which consists of the addition of a single monosaccharide (O-linked β -D-N-acetylglucosamine or O-GlcNAc) to hydroxyl groups of serine and/or threonine residues. The substrate for O-GlcNAcylation is uridine diphosphate- β -N-acetylglucosamine (UDP-GlcNAc), the end product of the hexosamine biosynthetic pathway (HBP), and its abundance controls the efficiency of protein O-GlcNAcylation. Approximately 2–5% of cellular glucose is diverted to the HBP, which is consequently strongly connected to the nutrient availability and carbohydrate metabolism (Wells et al., 2001, 2003b; Zachara and Hart, 2006; Zachara et al., 2015; Fisi et al., 2017). O-GlcNAc modification is reversible and specific and is tightly controlled by the activity of the enzymes O-GlcNAc-transferase (OGT) and O-GlcNAcase (OGA), which catalyze the addition and the removal of O-GlcNAc from target proteins, respectively (Gloster and Vocadlo, 2010; Yang and Qian, 2017).

O-GlcNAcylation may compete and establish a dynamic interplay with other post-translational modifications, including phosphorylation, by occurring on same sites or adjacent sites (Slawson and Hart, 2011). Amino acids that are either phosphorylated or O-GlcNAcylated in a mutually exclusive manner are called YinOYang sites and are crucially involved in controlling protein activity (Zeidan and Hart, 2010).

O-GlcNAcylation regulates a variety of cellular and molecular processes including intracellular signaling, gene transcription, protein–protein interaction, and stability, localization and expression of proteins (Butkinaree et al., 2010). Consequently, O-GlcNAc plays a role in numerous physiological and pathological conditions, including the response to stress, cancer, neurodegeneration, and diabetes mellitus (Wells et al., 2001; Zachara et al., 2004; Hart et al., 2007; Fardini et al., 2013). Specifically, strong positive correlations between protein O-GlcNAc levels and insulin resistance, glucose toxicity (McClain and Crook, 1996; Copeland et al., 2008), and chronic complications of diabetes mellitus (Brownlee, 2001; Buse, 2006; McLarty et al., 2013) have been well established in cell culture and animal models (Buse, 2006; Dias and Hart, 2007; Nagy et al., 2007) as well as in patients (Wang et al., 2009; Park et al., 2010; Springhorn et al., 2012; Myslicki et al., 2014; Pagesy et al., 2018). Among the multiple and diverse functions of O-GlcNAcylation, one of the least studied is the modulation of the regulation of cellular volume.

The regulation of cellular volume is a homeostatic reaction essential to normal cell function (Lang et al., 1998; Hoffmann et al., 2009). Variations of the cellular volume are due to an imbalance between the intra- and the extracellular osmolality; may induce alterations in cell morphology, function, and survival; and therefore require counterbalance. In mammalian cells, swelling activates a rapid release of KCl and/or non-essential organic osmolytes accompanied by cellular water (Jakab et al., 2002). This process is called regulatory volume decrease (RVD) and permits swollen cells to regain their original volume. The main conductive pathway leading to the release of Cl⁻ during

RVD is called IClswell (Furst et al., 2002a), and the respective main molecular entity was identified as the leucine-rich repeat containing protein 8A (LRRC8A) (Qiu et al., 2014; Voss et al., 2014; Pedersen et al., 2016), although other channels may also play a role in this context (Liu et al., 2019; Okada et al., 2019).

Our previous study established a link between O-GlcNAcylation and RVD. Increasing the cellular O-GlcNAc levels by a hour pretreatment with glucosamine, PUGNAc, or high glucose (30 mM) altered the response of Jurkat cells to a hypotonic stimulus. Specifically, the swelling observed following exposure of cells to a hypotonic extracellular medium was augmented and the intracellular water diffusion was reduced (Nagy et al., 2010). However, the molecular mechanism by which augmented O-GlcNAcylation affects RVD remains to be established.

ICln is a ubiquitous, highly conserved, multifunctional protein that plays a fundamental role in RVD (Paulmichl et al., 1992; Furst et al., 2006). During a hypotonic stimulus, ICln is transposed toward the plasma membrane and facilitates the activation of IClswell (Ritter et al., 2003; Dossena et al., 2011). Binding of cytosolic ICln to the intracellular domain of α -integrin is an essential prerequisite for ICln association with the plasma membrane and IClswell activation and requires a direct molecular interaction between highly conserved amino acid motifs of both proteins (Schedlbauer et al., 2019). Specifically, the sequence (61)ISLHA(65) (single-letter amino acid code; numbers refer to the amino acid position within the human ICln protein sequence), located in the β 4– β 5 loop and β 5 sheet of the pleckstrin homology-like N-terminal portion of ICln (Furst et al., 2005), appears to be essential for binding to α -integrin as well as for the ICln-induced activation of IClswell. Interestingly, ICln is O-GlcNAcylated (Hahne et al., 2013); however, the ICln O-GlcNAc modification site(s) as well as their physiological significance are not assessed.

The aim of the present study was to explore the mechanism by which O-GlcNAcylation affects RVD. Here, we show that augmented O-GlcNAcylation prevents RVD by reducing the magnitude of the ion current IClswell. IClswell inhibition results from O-GlcNAcylation of the protein ICln on serine 67, which prevents its binding to the intracellular domain of the integrin α chain. These findings suggest that dysfunction of cellular volume regulation may contribute to diseases associated with chronic elevation of O-GlcNAcylation.

MATERIALS AND METHODS

Cell Culture and Transfection

Human embryonic kidney (HEK) 293 Phoenix (DiCiommo et al., 2004) and HeLa cells [human cervical adenocarcinoma, CCL-2, obtained from American Type Cell Culture Collection (ATCC), Manassas, VA, United States] were cultured in Minimum Essential Eagle Medium (Sigma-Aldrich, St. Louis, MO, United States) supplemented with 10% fetal bovine serum (GIBCO, Thermo Fisher, Waltham, MA, United States), 2 mM L-glutamine, 100 U/ml penicillin, 100 μ g/ml streptomycin, and 1 mM pyruvic acid (sodium salt). NIH/3T3 cells (mouse

embryonic fibroblasts, CRL-1658, obtained from ATCC) were cultured in Dulbecco's Modified Eagle's Medium (Sigma-Aldrich) supplemented with 10% bovine calf serum (GIBCO), 100 U/ml penicillin and 100 µg/ml streptomycin. The cells were maintained at 37°C, 5% CO₂, 95% air, and 100% humidity. Subcultures were routinely established every second to third day by seeding the cells into 100-mm diameter Petri dishes following trypsin/ethylenediaminetetraacetic acid (EDTA) treatment.

For transfection, cells were seeded into six-well plates or 30-mm diameter Petri dishes, grown overnight to ~50% confluence, and transiently transfected with 1–3 µg of plasmid DNA by the calcium phosphate co-precipitation method (HEK 293 Phoenix) or 1.5–3 µg of plasmid DNA and 3–6 µl METAFACTENE PRO® (Biontex, Munich, Germany), following the manufacturer's instructions (HeLa and NIH/3T3). For co-transfection experiments, equimolar amounts of two vectors were used. Medium was replaced 6–8 h after transfection.

Plasmid Constructs

For electrophysiology experiments, the open reading frames (ORFs) coding for human ICl_n (hICl_n, NCBI Reference Sequence: NP_001284.1); *Canis familiaris* ICl_n (from Madin-Darby Canine Kidney cells, MDCK ICl_n, NP_001003288.1); and the long (OGA-L, NP_036347.1) or short (OGA-S, NP_001135906.1) isoforms of OGA, OGT (NP_858051.1; all from HEK 293 Phoenix cells), or integrin αIIbshort (amino acids 987–1039 of the human integrin αIIb chain, NP_000410.2) were cloned into the bicistronic mammalian expression vectors pIRES2EGFP or pIRES2dsRedExpress (Clontech, Mountain View, CA, United States). The use of a vector bearing the internal ribosome entry site (IRES) allows for the simultaneous expression of the protein of interest (either OGT, OGA, integrin αIIbshort, or ICl_n) and the transfection marker (either the enhanced green fluorescent protein EGFP or the red fluorescent protein dsRED) as two individual proteins from the same bicistronic mRNA, without the production of fusion proteins (Morgan et al., 1992). Control experiments were conducted in cells transfected with the pIRES2EGFP-EGFP vector, where an additional EGFP coding sequence was cloned into the pIRES2EGFP expression vector. Consequently, the control vector contained two EGFP coding sequences (one in the multiple cloning site and one downstream of the IRES sequence).

Plasmids encoding for ICl_n Ser67Ala, Thr223Ala, and Ser193* were obtained by site-directed mutagenesis of vectors bearing the wild-type ICl_n cDNA with the QuikChange Site-Directed Mutagenesis Kit (Agilent, Santa Clara, CA, United States). Mutagenesis primers were designed in-house (Gene Runner, version 5.0.993 Beta) and obtained from Microsynth AG (Balgach, Switzerland).

To produce fusion proteins for fluorescence resonance energetic transfer (FRET) experiments, hICl_n, MDCK ICl_n, hOGT, hOGA, or integrin αIIbshort ORFs were cloned into the pEYFPC1, pEYFPN1, pECFPC1, or pECFPN1 mammalian expression vectors (Clontech) in frame with the ORF of the enhanced yellow fluorescent protein (EYFP) or enhanced cyan fluorescent protein (ECFP).

All plasmid inserts were sequenced prior to their use in experiments (Microsynth AG).

Manipulation of O-GlcNAcylation of Cellular Proteins

To increase the O-GlcNAcylation levels of cellular proteins, cells were incubated for 1 h in complete medium with 20 mM D-glucose, 5 mM glucosamine, 100 µM O-(2-acetamido-2-deoxy-D-glucopyranosylidene)amino N-phenyl carbamate (PUGNAc; Sigma Aldrich), 100 µM PUGNAc, and 5 mM glucosamine (Nagy et al., 2010) or were transfected for 24 h with OGT. To reduce the O-GlcNAcylation levels of proteins, cells were transfected for 24 h with OGA. PUGNAc was dissolved in 100% dimethyl sulfoxide (DMSO) and stored at –20°C. To obtain equal osmolarity of control incubation media, 20 mM mannitol and 5 mM D-glucose were used instead of 20 mM D-glucose and 5 mM glucosamine.

Patch Clamp

Cells were transferred to glass coverslips (10-mm diameter) 8 h after transfection, and electrophysiology measurements were performed 24–32 h after transfection. Single cells expressing the transfection marker EGFP, dsRed, or both could be identified by fluorescence microscopy using FITC (excitation: 480/30x, dicroic: 505 dclp, and emission: 535/40 m) and TRITC (excitation: 540/25x, dicroic: 565 dclp, and emission: 605/55 m) filter sets. Selected cells were voltage-clamped using the whole-cell patch-clamp technique as previously described (Gandini et al., 2008; Dossena et al., 2011; Tamma et al., 2011; Morabito et al., 2017; Schedlbauer et al., 2019). The resistance of the glass pipettes was 3–8 MΩ when filled with the pipette solution (CsCl 125 mM, MgCl₂ 5 mM, EGTA 11 mM, ATP Mg²⁺ salt 2 mM, HEPES 10 mM, pH 7.2 adjusted with CsOH, and 300 mOsm/kg H₂O). Fast exchange of the isotonic bath solution (NaCl 125 mM, CaCl₂ 2.5 mM, MgCl₂ 2.5 mM, HEPES 10 mM, mannitol 40 mM, pH 7.4 adjusted with NaOH, and 300 mOsm/kg H₂O) with a hypotonic bath solution (NaCl 125 mM, CaCl₂ 2.5 mM, MgCl₂ 2.5 mM, HEPES 10 mM, pH 7.4 adjusted with NaOH, and 260 mOsm/kg H₂O) was obtained using a perfusion system with a flow rate of 5 ml/min and a bath volume of ~300 µl. For data acquisition, an EPC10 USB amplifier (HEKA Elektronik, Lambrecht, Germany) controlled by a Macintosh computer running the Patch Master (v2x32, HEKA Elektronik) software was used. Access resistance was monitored throughout the recordings and never exceeded thrice the recording electrode resistance. Fast and slow capacitance were compensated. All current measurements were filtered at 2.9 kHz and digitized at 50 kHz. To monitor the activation of the swelling-activated chloride current (ICl_{swell}), cells were held at 0 mV and step pulses of 400-ms duration were applied from 0 to 40 mV every 20 s. To establish the current to voltage (IV) relationship, step pulses of 500-ms duration were applied every 5 or 10 min from –120 to +100 mV in 20-mV increments from a holding potential of 0 mV. For data analysis, Fit Master (v2x32, HEKA Elektronik) and Excel (Microsoft, United States) software were used. The current values (pA) were normalized to the membrane capacitance (pF) to obtain the current density

(pA/pF). Each data set was obtained from cells from at least three independent subcultures with control experiments in cells of the same subculture.

Western Blotting

Cells were washed twice with ice-cold phosphate-buffered saline (PBS) and lysed on ice in a buffer containing 20 mM Tris-HCl, 150 mM NaCl, 1 mM EDTA, 0.1% NP40, and protease inhibitor cocktail (Roche, Basel, Switzerland). Subsequently, cellular debris was discarded by centrifugation at $16,000 \times g$ for 30 min at 4°C and the supernatant was collected. Typically, 10 µg of total proteins were separated by a 7.5% polyacrylamide gel containing 0.1% SDS and electroblotted using a polyvinylidene fluoride membrane (Bio-Rad, Basel, Switzerland) by applying a constant voltage (75 V) for 2 h at 4°C. Membranes were blocked for 1 h at room temperature in 5% bovine serum albumin (BSA) diluted in Tris-buffered saline (150 mM NaCl and 15 mM Tris-HCl) containing 0.1% Tween 20 (TBST) and incubated overnight at 4°C with the following primary antibodies: mouse monoclonal IgM CTD110.6 (Cell Signaling Technology, Inc., Danvers, MA, United States), highly specific for O-glycosylated proteins (Kneass and Marchase, 2004), diluted 1:1,000, or rabbit polyclonal IgG against amino acids 151–164 of CLNS1A (Sigma Aldrich), diluted 1:2,000. The housekeeping proteins GAPDH or β-actin were detected with a goat (GenScript, Piscataway, NJ, United States) or rabbit (Cell Signaling) polyclonal antibody, respectively, both diluted 1:1,000. Membranes were washed three times in TBST and incubated for 1 h at room temperature with the secondary antibodies diluted 1:10,000 in PBS and 5% BSA (goat anti-mouse IgM, IRD-680 RD, donkey anti-goat, IRD-800 CW, or goat anti-rabbit, IRD-800 CW, all from LI-COR, Lincoln, NE, United States). The signal of immunocomplexes was revealed using the Odyssey (LI-COR) infrared imaging system. Densitometric analysis was done using the ImageJ (1.49v) software.

Acceptor Photobleaching Fluorescence Resonance Energy Transfer

Cells were transferred to round 3-cm diameter glass slides 32 h post-transfection and fixed for 30 min with 4% paraformaldehyde in Hanks' Balanced Salt Solution (HBSS) 48 h post-transfection. Imaging was performed in HBSS at room temperature. The FRET acceptor EYFP was excited with the 514-nm line of the Argon laser, and the emission was detected in the 525–600-nm range. The FRET donor ECFP was excited with the 405-nm laser, and the emission was detected in the 450–490-nm range. Imaging was performed by sequential acquisition with FRET AB-Wizard with a Leica TCS SP5II AOBs confocal microscope (Leica Microsystems, Wetzlar, Germany) equipped with a HCX PL APO 63x/1.20 Lambda blue water immersion objective and controlled by the LAS AF software (version 2.7.3.9723, Leica Microsystems). EYFP photobleaching in whole cells was obtained with 15 sequential illuminations at 514 nm (zoom factor 8×). FRET efficiency was calculated using the following formula:

$$\text{FRET efficiency} = 1 - \text{ECFP}_{\text{pre}}/\text{ECFP}_{\text{post}} \quad (1)$$

ECFP_{pre} and ECFP_{post} refer to the ECFP intensity before and after EYFP photobleaching, respectively, and were determined either in the bleaching regions of interest (ROI) or in plasma membrane ROIs, as indicated. In the latter case, ROIs were drawn within the bleaching ROI, on the pre-bleaching EYFP image, in areas with a clear targeting of αIIb_s-EYFP at the cell periphery.

Cell Volume Measurements

Cell volume measurements were performed as previously described (Morabito et al., 2013, 2014, 2017). Briefly, HEK 293 Phoenix cells were transferred to round 3-cm diameter glass slides and successively placed in a perfusion chamber. Cell volume measurements were performed on cells sequentially exposed to the following: isotonic solution for 1 min and hypotonic solution (~15% reduction of osmolality by omission of mannitol) for 2–3 min. Cell volume measurements were performed on roundish cells. For each experiment, 100–150 images/cell (1 image/1,293 s) were taken with a phase contrast microscope (Leica DMI 6000, with a HCX PL APO 63x/1.20 Lambda blue water immersion objective; Leica Microsystems). Cell diameter was measured for each image and, assuming the cell as a sphere, cell volume was calculated and expressed as V/V_0 , where V and V_0 represent the volume of a cell at a given time and the average volume of the same cell in isotonic solution, respectively.

Immunoprecipitation and Mass Spectrometry

For immunoprecipitation, cells were lysed on ice for 30 min in IP buffer (25 mM Tris-HCl, pH 7.4, 150 mM NaCl, 1 mM EDTA, 1% Triton X-100, 5% glycerol, 0.05% Na-azide, protease inhibitor cocktail, and 50 µM of PUGNAc). Next, the samples were sonicated for 5 s at 30% power (Bandelin Sonopuls). Finally, the samples were centrifuged at 4°C for 10 min at 3,000 rpm, and the supernatants were incubated with anti-ICln antibodies #1 or #2 at 4°C overnight on a rotary shaker. Anti-ICln #1 is a polyclonal antibody raised in rabbits against amino acids 214–237 of human ICln, while anti-ICln #2 (Santa Cruz Biotechnology, Cat. No.: SC-393525) is a mouse monoclonal antibody. Protein A-Sepharose beads (Sigma-Aldrich) were prepared as follows: beads were washed in 800 µl IP buffer and incubated for 30 min in 3% BSA/IP buffer at 4°C on a shaker to block non-specific binding sites. Next, immunoprecipitates were incubated with the Protein A beads on a rotary shaker at 4°C for 3 h. Next, the beads were washed in 1 ml of IP buffer twice, the last wash buffer was removed carefully, and 50 µl of elution buffer (0.1 M glycine, pH 2.8) was added to the beads and incubated for 10 min at room temperature. The eluate (IP) was kept and 6 µl of 1.5 M Tris-HCl (pH 8.8) was added to neutralize the pH. During the process, lysates including the antibodies (input) and flow-through (FT) from the beads were collected. All of the collected samples (input, FT, and IP) were adjusted with 4X sample buffer and processed on 7.5% polyacrylamide gel electrophoresis. The proteins were either transferred to PVDF membranes for western blot analysis or the gel was directly

stained with Coomassie Brilliant Blue R-250 for further mass spectrometry analysis.

For mass spectrometry (MS), the protein bands of interest were cut out from the Coomassie-stained gels and digested by trypsin using the in-gel digestion protocol as described (Szabo et al., 2012). Briefly, excised gel bands were cut into small pieces, destained in 25 mM NH_4HCO_3 and 50% acetonitrile, dehydrated with acetonitrile, and dried. The gel pieces were rehydrated in 12.5 ng/ μl trypsin (Promega, Madison, WI, United States) solution (in 25 mM NH_4HCO_3) and incubated overnight at 37°C. Peptides were extracted with 5% formic acid and twice with 60% acetonitrile in 1% formic acid.

Digested protein samples were analyzed using a Waters nanoACQUITY UPLC System coupled with a Thermo Q Exactive plus mass spectrometer. Forty-five-minute long gradients from 3% to 40% acetonitrile/water were applied on a Waters BEH130 C18 75 μm \times 100 mm column with 1.7 μm particle size C18 packing. The mass spectrometer was operated in DDA mode, and the 12 most intensive peptides were selected for fragmentation in each MS scan.

From all acquired data, peaklists were generated by the Msconvert tool from ProteoWizard (Chambers et al., 2012). All MS/MS samples were analyzed using Mascot 2.2.06 (Matrix Science, London, UK). Mascot was set up to search the UniProt Human proteome database (2017.03 release, 70,942 entries) assuming digestion by trypsin and allowing up to two missed cleavage sites. Database searching was carried out with a fragment ion mass tolerance of 0.1 Da and a parent ion tolerance of 10 ppm. The iodoacetamide derivative of cysteine was specified as a fixed modification, and oxidation of methionine, N-acetyl-glycosylation of serine and threonine, acetylation of protein N-terminal, and formylation of peptide N-terminal were specified as a variable modification in Mascot. Database search results were validated, and MS/MS spectra were annotated in PeptideShaker 1.16.45 (Vaudel et al., 2015).

Immunocytochemistry

HeLa cells were grown on coverslips until ~50% confluence and treated with either 100 μM PUGNAc and 5 mM glucosamine or the vehicle for 1 h at 37°C. Following this, the cells were exposed to 300 mOsmol isotonic (mannitol 100 mM, NaCl 87.5 mM, CaCl_2 2.5 mM, MgCl_2 2.5 mM, HEPES 10 mM, pH 7.4) or 200 mOsmol hypotonic (NaCl 87.5 mM, CaCl_2 2.5 mM, MgCl_2 2.5 mM, HEPES 10 mM, pH 7.4) solution for 15 min. Next, cells were fixed in 10 v/v% PBS-buffered formaldehyde for 30 min at room temperature. To avoid formaldehyde autofluorescence, the coverslips were quenched with 50 mM ammonium chloride for 10 min. The cells were permeabilized with 0.25 v/v% Triton-X 100 for 10 min. Non-specific sites were blocked with 5% bovine serum albumin (Sigma-Aldrich) in PBS for 30 min, and then, the coverslips were incubated at room temperature with the primary antibodies in 5 w/v% BSA/PBS for 2 h. The primary antibodies and their dilutions were the following: CTD110.6 (1:200) and rabbit anti-ICln (1:100). After rinsing three times with PBS, samples were incubated with the corresponding secondary

antibodies for 1 h in the dark. Finally, coverslips were mounted with VECTASHIELD (Vector Laboratories, Burlingame, CA, United States) mounting medium. Image acquisition was performed with a Zeiss LSM 710 confocal scanning microscope (Carl Zeiss AG, Oberkochen, Germany) equipped with the ZEN software (ver2.3, Carl Zeiss AG, Oberkochen, Germany) and a 63 \times objective. Alexa Fluor 488 (ICln) and Texas Red (CTD110.6) fluorescence channels were used for image acquisition (excitation 488 and 594 nm, emission 518 and 624 nm, respectively).

Bioinformatic Analysis

The amino acid sequence of human ICln (NP_001284.1) was analyzed with the YinOYang WWW server (<http://www.cbs.dtu.dk/services/YinOYang/>), which produces neural network predictions for O- β -GlcNAc attachment sites in eukaryotic protein sequences (Gupta and Brunak, 2002). This server can also use NetPhos, which predicts serine, threonine, or tyrosine phosphorylation sites in eukaryotic proteins, to identify possible phosphorylated sites that, when coinciding with O-GlcNAcylation sites, represent “YinOYang” sites (Blom et al., 2004). In addition, the *GlycoMine* (<http://glycomine.erc.monash.edu/Lab/GlycoMine/>) bioinformatics tool was used to predict O-linked glycosylation (Li et al., 2015).

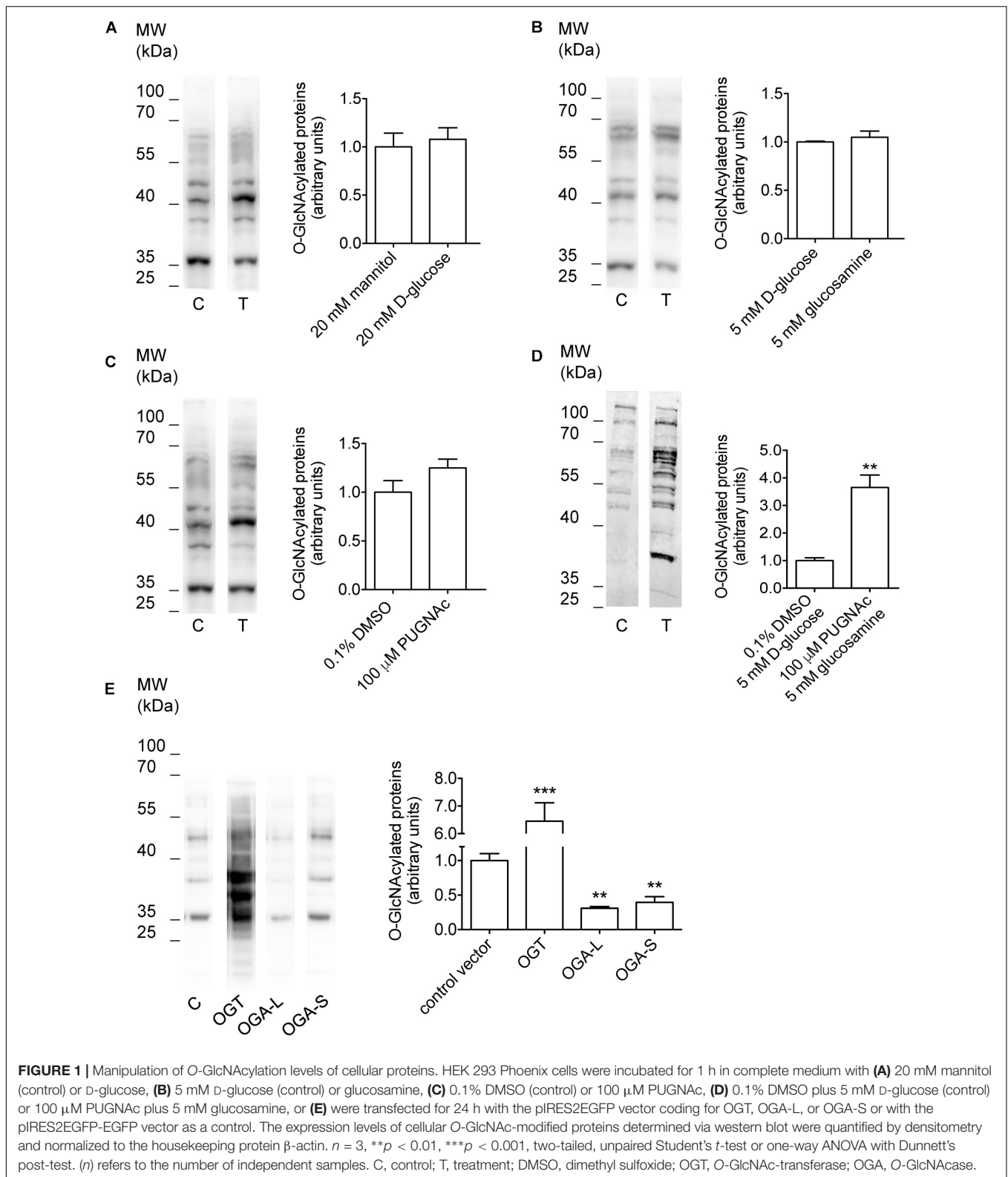
Statistical Analysis

All data are expressed as arithmetic means \pm standard errors of the mean. For statistical analysis and graphics, GraphPad Prism (version 5.0b for Mac OS, San Diego, CA, United States) and Excel (Microsoft) software were used. Significant differences between mean values were determined by the unpaired Student's *t*-test or ANOVA with Bonferroni's or Dunnett's post-test, as appropriate. Statistically significant differences were determined at * $p < 0.05$, ** $p < 0.01$, *** $p < 0.001$; (*n*) corresponds to the number of independent measurements.

RESULTS

Manipulation of O-GlcNAcylation of Cellular Proteins

Incubation of cells with O-GlcNAc precursors such as D-glucose or glucosamine, pharmacological inhibition of OGA with PUGNAc, as well as overexpression of OGT or OGA have formerly been used to experimentally increase or decrease O-GlcNAcylation levels of cellular proteins (Champattanachai et al., 2008; Yuzwa and Vocadlo, 2014; Ferron et al., 2018). Here, incubation of HEK 293 Phoenix cells for 1 h with 20 mM D-glucose, 5 mM glucosamine, or 100 μM PUGNAc failed to significantly increase O-GlcNAcylation levels of cellular proteins (Figures 1A–C and Table 1). However, combining 100 μM PUGNAc with 5 mM glucosamine increased O-GlcNAcylation up to 3.6-fold of control levels (Figure 1D and Table 1). Transfection of cells with OGT was the most effective maneuver and increased O-GlcNAcylation of 6.5-fold compared to cells



transfected with a control vector (Figure 1E and Table 1). Conversely, cells expressing either OGA-L or its splicing variant OGA-S showed a significant reduction in O-GlcNAcylation

of cellular proteins, which was more pronounced with OGA-L (Figure 1E and Table 1). Hence, the catalytic activity of OGA-S was found to be lower than that of OGA-L

TABLE 1 | Effect of manipulation of O-GlcNAcylation of cellular proteins on the current IClswell.

Treatment	% variation in O-GlcNAcylation	Effect on IClswell		
		Native cells	Cells transfected with IClN wild type	Cells transfected with IClN Ser67Ala
20 mM D-glucose	+8% (n.s.)	n.s.	n.s.	n.p.
5 mM glucosamine	+5% (n.s.)	n.s.	n.s.	n.p.
100 μ M PUGNAc	+25% (n.s.)	n.s.	n.s.	n.p.
100 μ M PUGNAc plus 5 mM glucosamine	+265%	n.s.	-55%	n.s.
OGT	+545%	-38%	-58%	-38%
OGA-S	-60%	n.s.	n.p.	n.p.
OGA-L	-69%	n.s.	+158%	n.s.

The % variation in O-GlcNAcylation was calculated from western blot data shown in **Figure 1**. The % variation in IClswell intensity was calculated at +100 mV. + and - denote an increase and decrease compared to the corresponding control, respectively. n.s., not significant; n.p., not performed.

(Kim et al., 2006). Therefore, only OGA-L was used in further experiments.

Increased O-GlcNAcylation of Cellular Proteins Inhibits the Endogenous IClswell Current

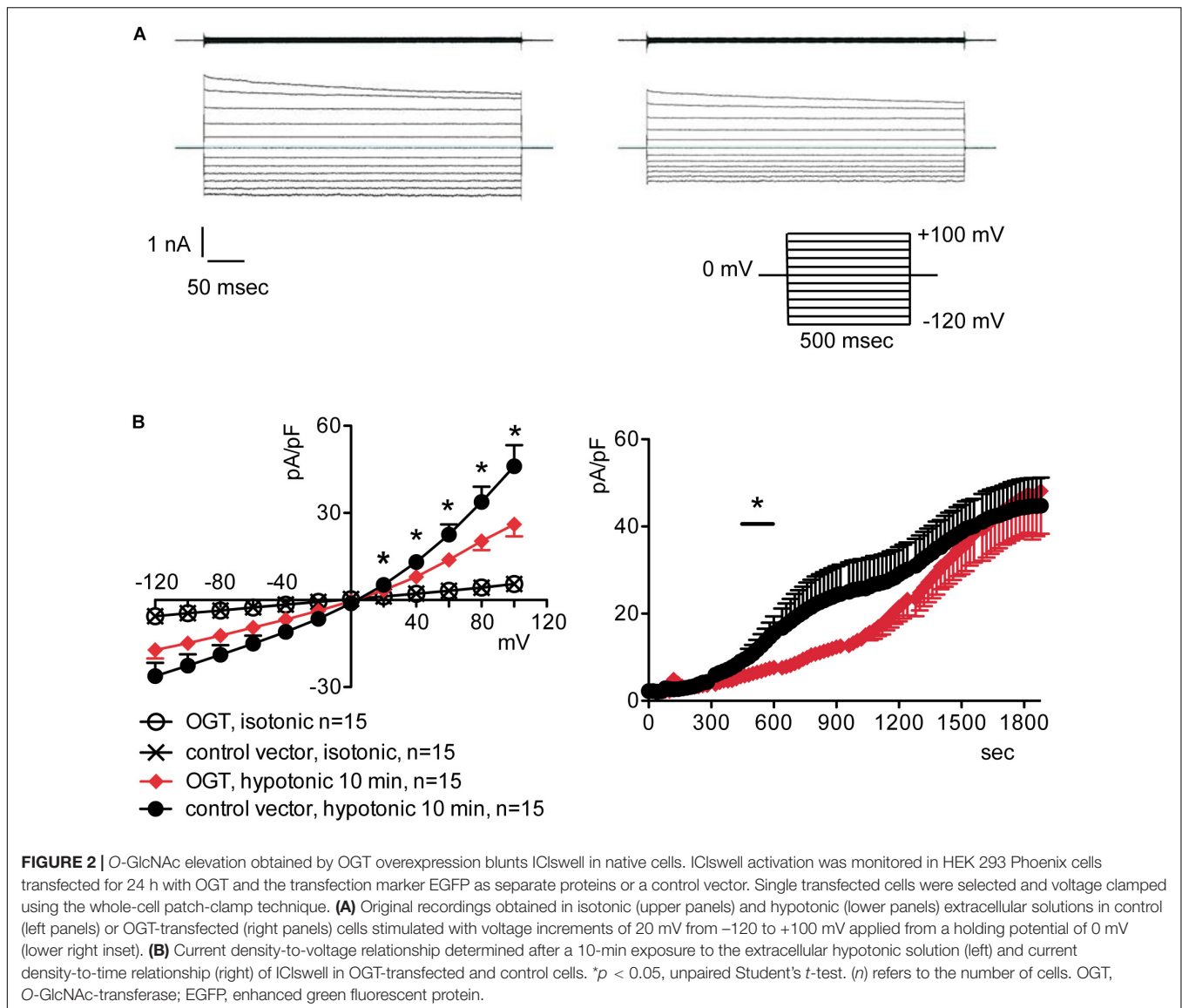
To assess the possible influence of O-GlcNAc on the endogenous swelling-activated chloride current IClswell, the patch-clamp technique in whole-cell configuration was used in untransfected cells in which the O-GlcNAcylation of cellular proteins was experimentally increased or decreased. Cells were initially kept in an extracellular isotonic solution. In these conditions, currents were very small and undistinguishable from leakage currents. Exposure of cells to an extracellular hypotonic solution activated a current with outward rectification and slow time-dependent inactivation at voltages higher than +40 mV. The reversal potential (E_{rev}) of this current was 0 mV, which corresponds to the equilibrium potential of chloride with the experimental solutions used and is therefore indicative of a chloride selective current (**Supplementary Figure S1**). All of the above-mentioned characteristics represent the biophysical fingerprints of IClswell (Furst et al., 2002a). Pre-incubation of HEK 293 Phoenix cells for 1 h with 20 mM D-glucose, 5 mM glucosamine, or 100 μ M PUGNAc failed to increase O-GlcNAcylation of cellular proteins (**Figures 1A–C**) and did not modify the endogenous IClswell current (**Supplementary Figures S1–S3 and Table 1**). Pre-incubating cells with 100 μ M PUGNAc plus 5 mM glucosamine, which was effective in increasing O-GlcNAcylation levels in these cells (**Figure 1D**), also did not significantly modify the endogenous IClswell current (**Supplementary Figure S4 and Table 1**). In contrast, in cells transfected with OGT, which was twice as effective as 100 μ M PUGNAc plus 5 mM glucosamine in increasing O-GlcNAcylation levels, IClswell magnitude was significantly reduced and the activation in time was delayed in comparison to control conditions (**Figure 2 and Table 1**). In cells transfected with OGA-L, IClswell showed a tendency to an increase, which, however, was not statistically significant (**Supplementary Figure S5**).

Increased O-GlcNAcylation of Cellular Proteins Inhibits the IClN-Induced IClswell Current

Overexpression of the heterologous protein IClN up-regulates IClswell in several cell types (Paulmichl et al., 1992; Hubert et al., 2000; Furst et al., 2002b; Dossena et al., 2011; Schedlbauer et al., 2019) (**Supplementary Figure S6**). In these cells, the apparent IClswell is the sum of the endogenous IClswell and the IClN-induced IClswell. Similarly to what was observed for the endogenous IClswell current, pre-incubation of cells with 20 mM D-glucose, 5 mM glucosamine, or 100 μ M PUGNAc failed to modify IClswell in IClN-transfected cells (**Supplementary Figures S7–S9 and Table 1**). In contrast, treatment with 100 μ M PUGNAc plus 5 mM glucosamine, as well as OGT overexpression, significantly inhibited IClswell (**Figures 3, 4 and Table 1**). As 5 mM glucosamine plus 100 μ M PUGNAc had no effect on the endogenous current, the 55% inhibition of IClswell that was observed in IClN-transfected cells (**Table 1**) must have arisen from inhibition of the IClN-induced current. Similarly, the OGT-induced IClswell inhibition in IClN-transfected cells (58%) most likely represents the sum of inhibition of (i) the endogenous IClswell (38%, **Table 1**) and (ii) the IClN-induced current. Conversely, IClswell was significantly up-regulated by OGA-L in IClN-transfected cells (**Figure 5 and Table 1**).

Increased O-GlcNAcylation of Cellular Proteins Prevents RVD

To assess the effects of an increased O-GlcNAcylation on RVD, HEK 293 Phoenix cells were treated with 100 μ M PUGNAc plus 5 mM glucosamine or 0.1% DMSO plus 5 mM glucose as control. The cell size was monitored before and during an osmotic stress, and cell volume changes were expressed as V/V_0 . As expected, the hypotonic shock promptly induced cell swelling followed by RVD activation in control cells, which regained their original volume. In contrast, in cells treated with 100 μ M PUGNAc and 5 mM glucosamine, cell swelling was more prominent and, importantly, was not followed by an RVD phase (**Figure 6**).



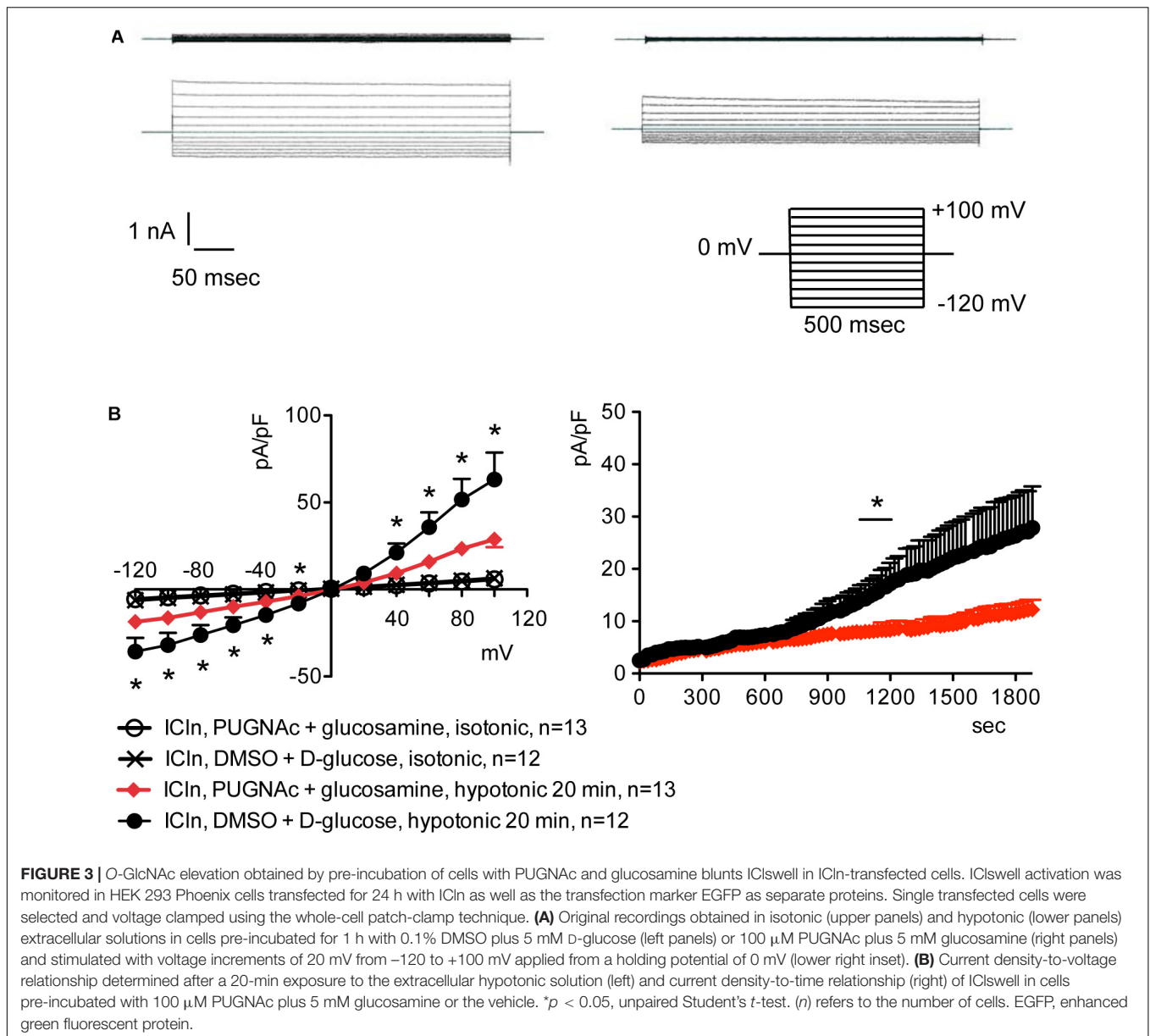
The C-Terminus of ICln Is O-GlcNAc Modified

Mass spectrometry was used to identify the ICln amino acids that are O-GlcNAcylated. After overexpressing ICln in HEK 293 Phoenix cells and treating the cells with 100 μ M PUGNAc and 5 mM glucosamine, we successfully identified the ICln protein from immunoprecipitated samples with up to 90% sequence coverage. Out of the 32 individual peptides found, we detected O-GlcNAc modification on peptide 187–205. **Figure 7A** reports the analysis of the charge state 3+ of this peptide. The O-GlcNAc-modified peptide has a mass/charge (m/z) value of 754.014 while its unmodified counterpart has an m/z value of 696.3258. **Supplementary Figure S10** demonstrates the analysis of the same peptide with a charge state of 2+. Unfortunately, no b- or y-ions that carried the O-GlcNAc modification could be found; therefore, the exact O-GlcNAc site could not be discerned (there are four Ser representing potential O-GlcNAcylation sites on

this peptide, **Figure 7B**). However, it is worth noting that both analyses found peaks that corresponded to the m/z value of GlcNAc residues and probably resulted from a loss of GlcNAc from the parent ion. In addition, we detected phosphorylation at Ser223 on peptide 206–236 (**Figure 7B**).

O-GlcNAcylation of the C-Terminus of ICln Is Not Involved in Modulating IClswell

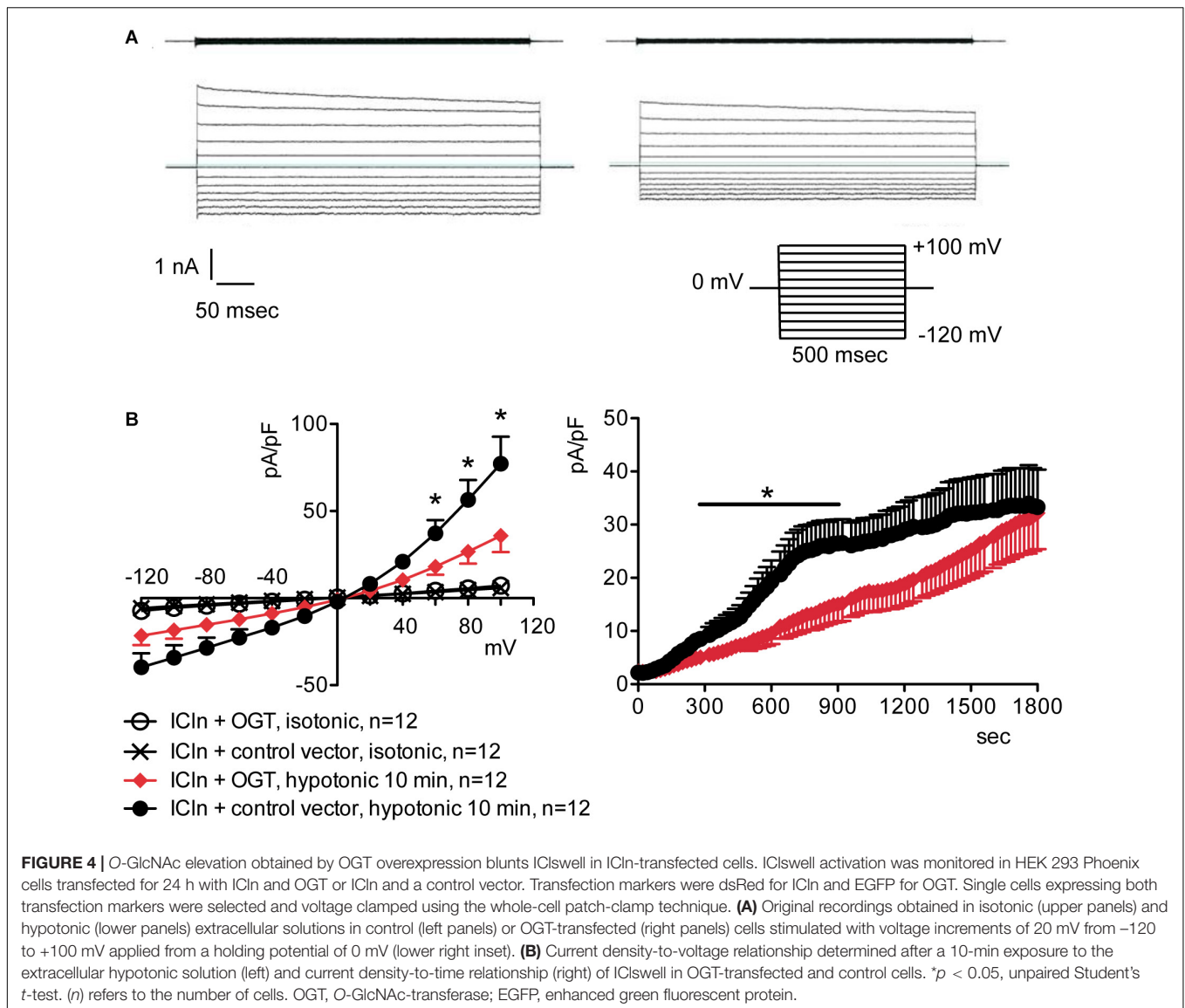
Based on the MS results, two mutations were designed in order to prevent ICln O-GlcNAcylation, i.e., Ser193* (nucleotides coding for Ser193 were substituted by a STOP codon) and Thr223Ala (**Figure 7B**). The first mutation leads to an early termination of translation with consequent protein truncation. The mutant protein lacks all O-GlcNAcylation sites, including Ser193. Thr223 is a phosphorylated amino acid with high likelihood of O-Glycosylation (**Supplementary Figures S11, S12**)



and therefore a potential YinOYang site. The second mutation converts this amino acid in the non-modifiable Ala. First, the expression of the ICln mutants and their ability of up-regulating IClswell were verified. Subsequently, the effect of an increased O-GlcNAcylation of cellular proteins was probed on the mutant ICln-induced current.

ICln expression in cells transfected with ICln Thr223Ala and Ser193* was doubled compared to the expression of the endogenous ICln in untransfected cells and was indistinguishable from that of cells transfected with wild-type ICln (Figure 8A). ICln Thr223Ala was fully functional, i.e., able of up-regulating IClswell to the level of ICln wild type (Figure 8B). In contrast, ICln Ser193* lost most of its activity, and only a small residual current, which was above the level of the endogenous IClswell, could be measured in transfected cells (Figure 8C).

Similarly to what was observed for the wild-type ICln-induced current, the ICln Thr223Ala-induced IClswell, as well as the residual ICln Ser193*-induced current, were inhibited by increases in the O-GlcNAcylation of cellular proteins induced by incubation of cells with PUGNAc and glucosamine (Figure 9). As pre-incubation of cells with PUGNAc plus glucosamine had no effect on the endogenous IClswell (Supplementary Figure S4), the inhibitory effect observed in cells transfected with ICln Thr223Ala or ICln Ser193* must arise from inhibition of the mutant ICln-induced current. These data clearly show that O-GlcNAcylation of ICln on Ser193 or Thr223 is not involved in suppressing IClswell and strongly suggest that the O-GlcNAcylation site involved in controlling the ICln-induced current is located upstream of Ser193.



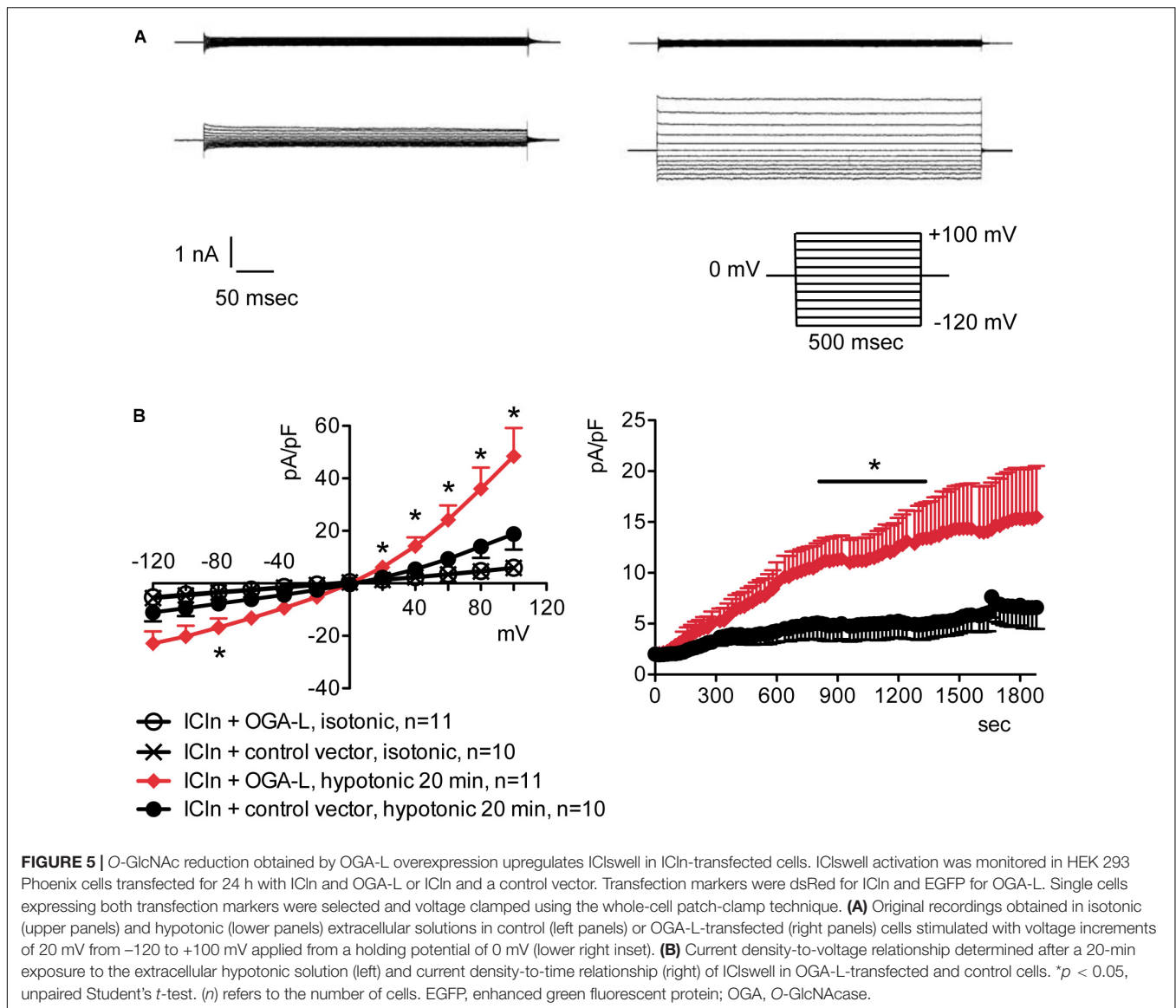
Ser67 Confers to IClN Sensitivity to O-GlcNAcylation

Upstream of IClN Ser193, there is a predicted YinOYang site at Ser67 (**Supplementary Figure S11**). This latter site is of particular interest as it lies in close proximity to the (61)ISLHA(65) motif, which is crucially involved in IClN binding to the intracellular domain of α -integrin and controls IClN function (Schedlbauer et al., 2019). Therefore, we decided to determine whether this site is involved in modulating IClN function following variation of O-GlcNAc levels. IClN Ser67Ala is fully functional, i.e., capable of up-regulating IClswell to an extent indistinguishable from that of wild-type IClN (**Figure 8D**). However, the current induced by this IClN mutant is insensitive to increases or decreases in the O-GlcNAcylation of cellular proteins (**Figure 10**). In particular, OGT overexpression induced a non-significant decrease (38%) in IClswell (**Figure 10B** and **Table 1**), which reflected the inhibition of the endogenous current (**Figure 2** and **Table 1**).

These experiments strongly suggest that O-GlcNAcylation of IClN at Ser67 inhibits IClswell.

IClN Interacts With OGT

Conjugation of O-GlcNAc to a protein requires a direct molecular interaction with OGT. To study this phenomenon, FRET between OGT and IClN was measured. This technique requires the transfection of the proteins of interest fused to fluorophores serving as the FRET donor and acceptor. In this study, ECFP and EYFP were used as the FRET donor and acceptor, respectively. EYFP fusion to the N-terminus of OGT did not affect its catalytic activity (**Figure 11A**) and was therefore used in experiments. EYFP-OGT gave a significant FRET with IClN-ECFP, which was reduced following mutation of Ser67. In contrast, FRET between EYFP-OGA and IClN did not exceed the stochastic FRET of the negative control. These results indicate that, in unstimulated cells, IClN preferentially interacts with OGT rather than OGA,

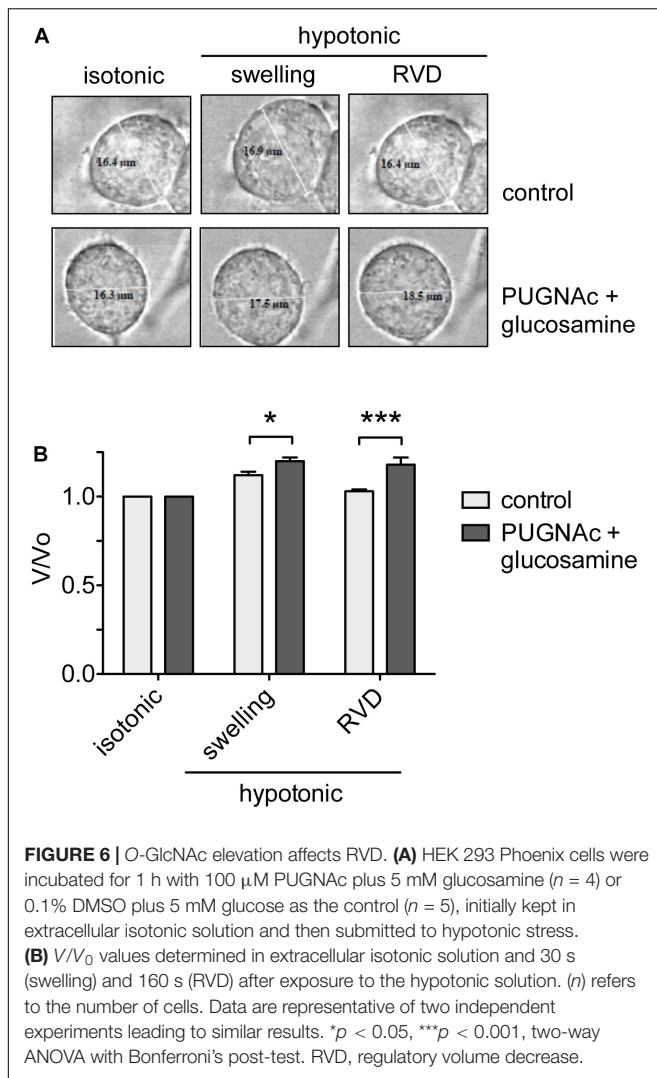


thus suggesting that ICln is constitutively O-GlcNAcyated. The ICln-OGT interaction is destabilized by mutation of Ser67, which may therefore represent the ICln O-GlcNAcylation site. The relatively small signal-to-noise ratio of ICln-OGT FRET indicates that the interaction between the two proteins is dynamic and transient, which is consistent with the characteristics of a reversible interaction between an enzyme and its target.

O-GlcNAcylation of ICln at Ser67 Prevents Its Interaction With α -Integrin

ICln establishes a direct molecular interaction with the intracellular domain of α -integrin (Larkin et al., 2004, 2009; Daxecker et al., 2008) (Figure 12), and perturbation of this interaction affects IClswell activation (Schedlbauer et al., 2019). Surprisingly, the interaction between the non-glycosylatable/non-phosphorylatable ICln Ser67Ala and α IIb integrin measured by FRET was stronger than the interaction

between wild-type ICln and α IIb integrin (Figure 12B). This finding suggests that post-translational modification of Ser67 weakens the binding of ICln to α -integrin. To further substantiate this hypothesis, the interaction between wild type and Ser67Ala ICln was measured following increases or decreases in the O-GlcNAcylation of cellular proteins obtained by incubation of cells with PUGNAc and glucosamine or transfection with OGA-L, respectively. In line with the hypothesis, elevation of O-GlcNAcylation reduced the FRET between wild-type ICln and α -integrin but, importantly, did not affect the FRET between Ser67Ala ICln and α -integrin (Figure 12C). This confirms that O-GlcNAcylation of Ser67 reduces the ICln/integrin interaction and further suggests that a fraction of the ICln protein pool is constitutively O-GlcNAcyated. In line with these hypotheses, reduction of O-GlcNAcylation increased the FRET between wild-type ICln and α -integrin. Again, Ser67Ala ICln was unresponsive to O-GlcNAcylation changes (Figure 12D).



Hypotonicity Reduces O-GlcNAcylation of Cellular Proteins

To assess the dynamic nature of protein O-GlcNAc modification upon direct changes during cell volume regulation, we exposed HeLa cells to 200 mOsmol hypotonic challenge. As shown in **Figure 13**, hypotonicity significantly reduced the fluorescence intensity corresponding to O-GlcNAc levels. Interestingly, this effect was also detected when O-GlcNAc levels were previously elevated by PUGNAc and glucosamine treatment.

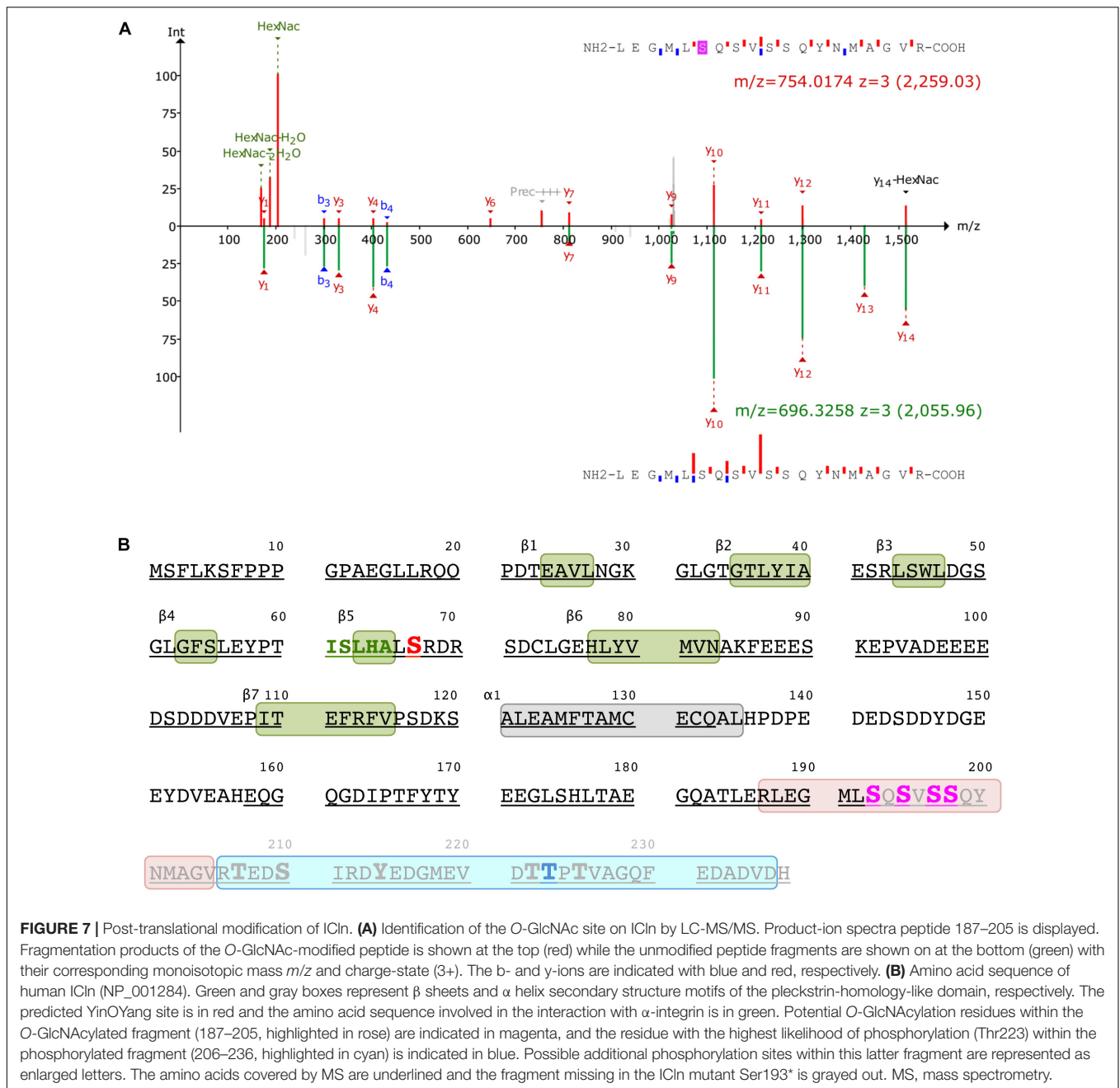
DISCUSSION

Since the discovery of O-GlcNAc modification, more than ~4,000 protein targets have been identified (Ma and Hart, 2014). A large number of O-GlcNAcylated proteins are involved in the regulation of many cellular events, including intracellular signaling, gene transcription, cellular metabolism, and stress responses (Butkinaree et al., 2010; Hart, 2014); therefore, it is not surprising that improper O-GlcNAcylation contributes

to the development of disease (Hart et al., 2011). Indeed, O-GlcNAcylation is associated with an increasing number of pathological states, such as type II diabetes mellitus, diabetic complications (Vaidyanathan and Wells, 2014; Peterson and Hart, 2016), insulin resistance (Wells et al., 2003a), cancer (Stowell et al., 2015), and neurodegeneration (Lagerlof and Hart, 2014; Banerjee et al., 2016; Hart, 2019). Therefore, uncovering the involvement of O-GlcNAcylation in a given pathological process and the identification of the respective protein targets could open the way to novel therapeutic strategies.

The alteration of RVD by increases in the O-GlcNAcylation of cellular proteins was first reported in Jurkat cells, an immortalized line of human T lymphocytes (Nagy et al., 2010). In this study, exposure of cells for 1 h to 30 mM D-glucose or 5 mM glucosamine was sufficient to significantly alter the levels of O-GlcNAcylated proteins as well as the osmotic response of cells to hypotonicity, leading to an increased swelling and delayed RVD. In HEK 293 Phoenix cells, significant increases in O-GlcNAc levels required incubation with 100 μ M PUGNAc plus 5 mM glucosamine for 1 h (**Figure 1D**). In agreement with the above-mentioned study, these cells swelled more than control cells when stimulated by hypotonicity, and their RVD was abrogated (**Figure 6**). These data show that alteration of osmotic resistance by increases in the O-GlcNAcylation of cellular proteins is not a feature restricted to Jurkat cells and consists of two components, i.e., increased swelling and inefficient or absent RVD. Jurkat cells seem more sensitive to O-GlcNAc precursors than HEK 293 Phoenix cells. This may be linked to differential expression of glucose transporters and/or metabolic enzymes and particularly to the very high expression of the sodium-glucose co-transporter SGLT2 and the glucose transporter GLUT1 in Jurkat cells (Kaji et al., 2018), which may drive efficient glucose intake in these cells.

Inefficient RVD following increases in the O-GlcNAcylation of cellular proteins was linked to reduced intracellular water diffusion (Nagy et al., 2010). During RVD, K^+ , Cl^- , and other intracellular osmolytes are lost, generating an osmotic water efflux that permits cells to reduce their volume (Friedrich et al., 2006). As water follows ions, one may speculate that reduced intracellular water diffusion may arise from impaired ion fluxes. Accordingly, pharmacological inhibition of swelling-activated ion channels leads to increased cell swelling after hypotonic stress and prevents RVD (Furst et al., 2002a), thus mimicking the effect of an increased O-GlcNAcylation. Therefore, we hypothesized that O-GlcNAcylation may alter RVD by inhibiting ion transport. The finding that the protein ICl_n, essential in the activation of the swelling-activated Cl^- current ICl_{swell}, is O-GlcNAc-modified (Hahne et al., 2013) further corroborated this hypothesis. As expected, incubation of cells for 1 h with 100 μ M PUGNAc plus 5 mM glucosamine significantly inhibited the ICl_n-induced ICl_{swell} (**Figure 3**), with no effect on the endogenous ICl_{swell} (**Supplementary Figure S4**). Further increase in O-GlcNAcylation obtained by OGT overexpression inhibited both the ICl_n-induced current and the endogenous ICl_{swell} current (**Figures 2, 4**). These findings suggest that the majority of endogenous ICl_n is O-GlcNAcylated in basal conditions and consequently unresponsive to relatively mild



increases in O-GlcNAcylation, while heterologous ICl_n is largely unmodified. Experimental conditions that did not significantly increase the O-GlcNAcylation levels of cellular proteins as assessed by western blot (Figures 1A–C) failed to suppress the ICl_n-induced current (Supplementary Figures S7–S9) as well as the endogenous ICl_{swell} current (Supplementary Figures S1–S3).

The identification of the O-GlcNAcylated proteins and O-GlcNAcylated residues of a protein can be challenging. O-GlcNAc modifications have low stoichiometry and generally low abundance, and the extremely labile nature of O-GlcNAc makes the determination of modification sites by conventional

tandem MS (MS/MS) difficult (Wang et al., 2014). Anti-O-GlcNAc antibodies did not recognize ICl_n immunoprecipitated from HEK 293 Phoenix cells, even following elevation of O-GlcNAc levels (data not shown). Therefore, computational methods remain an extremely useful tool in the identification of potential O-GlcNAcylation sites (Jia and Zuo, 2018). While MS evidenced that ICl_n is O-GlcNAc modified on its C-terminus, this is unlikely involved in the suppression of the ICl_n-induced current, as mutation or deletion of the C-terminus did not abrogate responsiveness of the ICl_n-induced current to O-GlcNAc elevation (Figure 9). Therefore, we assume that the ICl_n O-GlcNAcylated site

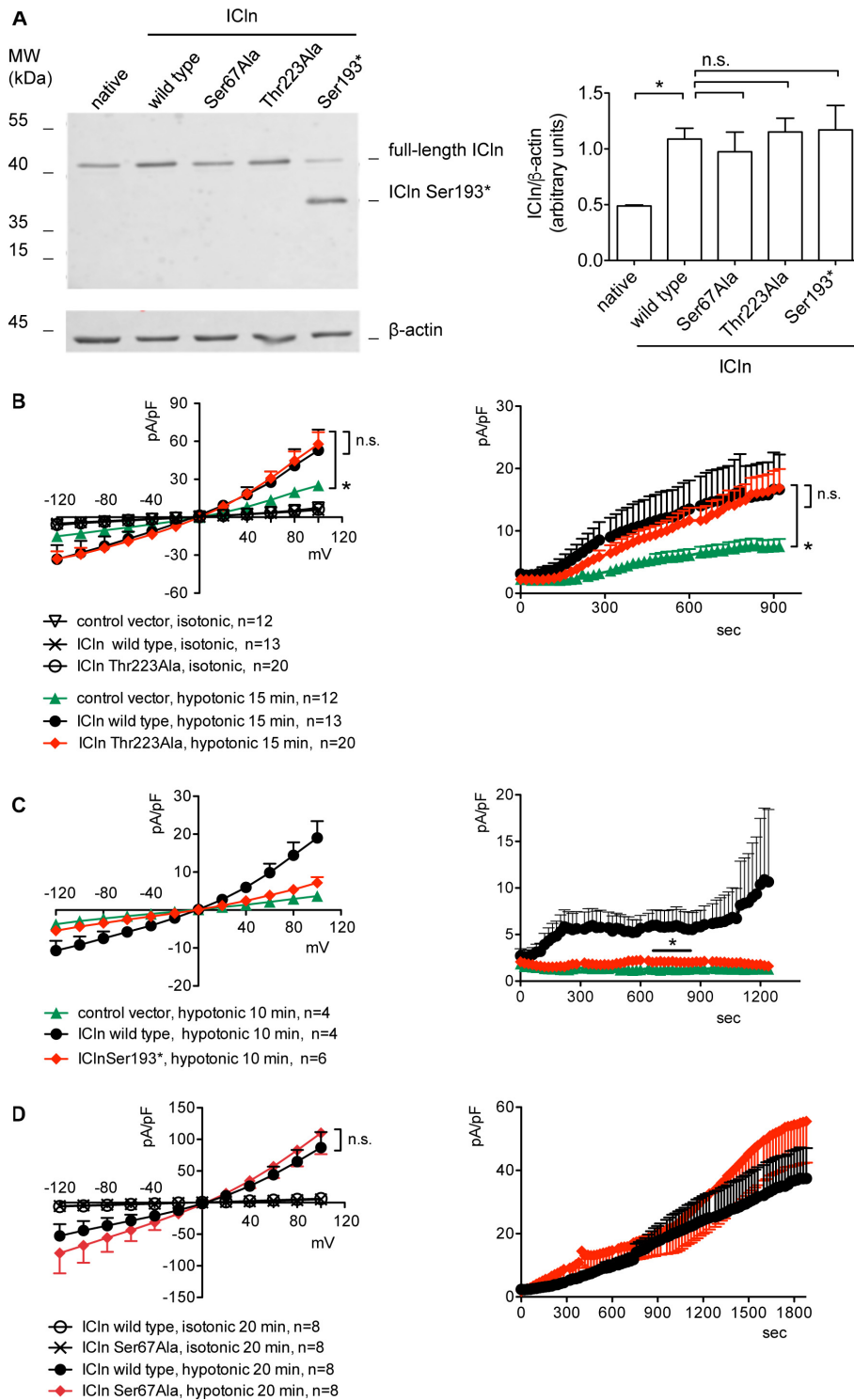


FIGURE 8 | Expression and function of ICln mutants. **(A)** HEK 293 Phoenix cells were transfected for 24 h with the indicated ICln mutants, wild-type ICln, or left untransfected. The expression levels of ICln determined via western blot (left panel) were quantified by densitometry and normalized to the housekeeping protein β -actin (right panel). $n = 3$ independent samples, $*p < 0.05$, one-way ANOVA with Dunnett's post-test. **(B–D)** ICln activation was monitored in HEK 293 Phoenix cells transfected for 24 h with wild-type or mutant ICln or a control vector, as indicated. Single transfected cells were selected based on the fluorescence of the transfection marker EGFP and voltage clamped using the whole-cell patch-clamp technique. The current density-to-voltage relationship (left panels) and the current density-to-time relationship (right panels) determined after exposure to the extracellular hypotonic solution are shown. $*p < 0.05$, unpaired Student's t -test. n.s., not significant. (n) refers to the number of cells. EGFP, enhanced green fluorescent protein.

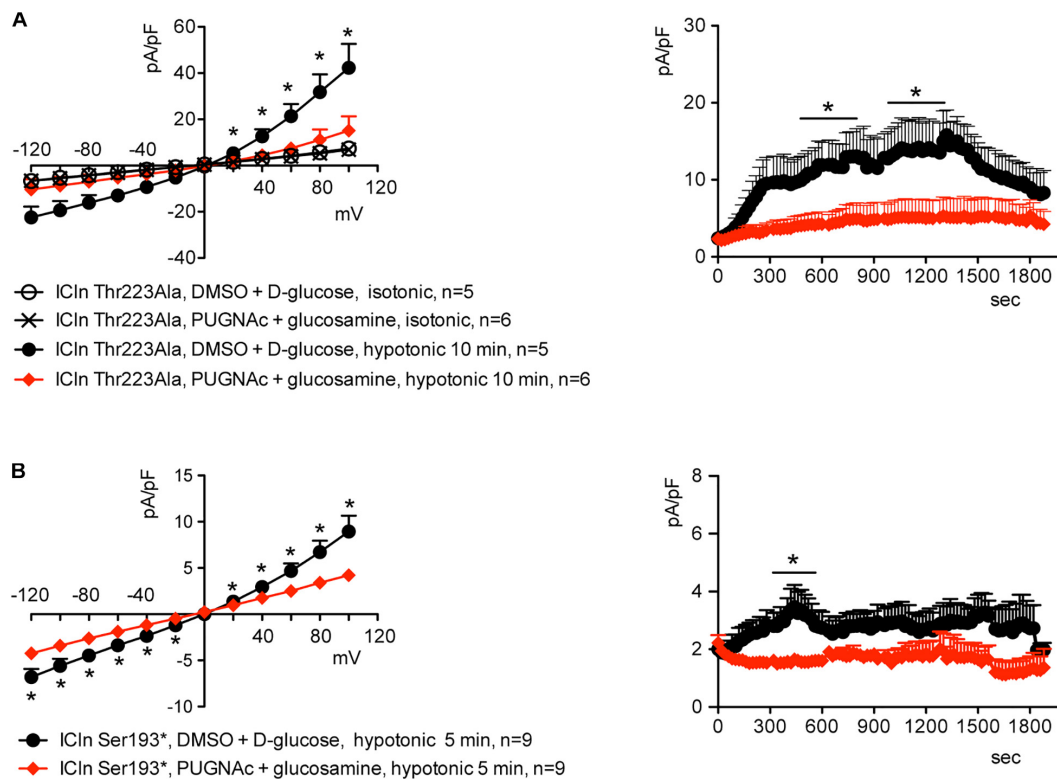


FIGURE 9 | O-GlcNAc elevation inhibits IClswell in cells transfected with non-O-glycosylatable forms of ICl. IClswell activation was monitored in HEK 293 Phoenix cells transfected for 24 h with **(A)** ICln Thr223Ala or **(B)** ICln Ser193* as well as the transfection marker EGFP as separate proteins and pre-incubated for 1 h with 100 μ M PUGNAc plus 5 mM glucosamine or 0.1% DMSO plus 5 mM D-glucose as the control. Single transfected cells were selected and voltage clamped using the whole-cell patch-clamp technique. The current density-to-voltage relationships determined in an extracellular hypotonic solution (left) and the current density-to-time relationships (right) of IClswell in cells pre-incubated with 100 μ M PUGNAc plus 5 mM glucosamine or the vehicle are shown. * $p < 0.05$, unpaired Student's *t*-test. (*n*) refers to the number of cells. EGFP, enhanced green fluorescent protein.

involved in the inhibition of the ICln-induced current could not be detected by MS as the O-GlcNAc moiety was most likely lost during sample preparation. In line with this hypothesis, mutation of the predicted YinOYang site on Ser67 conferred resistance of the ICln-induced current to O-GlcNAc increases or decreases (Figure 10), strongly suggesting that ICln is O-GlcNAc modified at Ser67. The non-significant 38% decrease in the ICln Ser67Ala-induced current observed in cells transfected with OGT most likely reflected the effect of O-GlcNAc elevation on the endogenous ICln (Figure 10B and Table 1).

The identification of a direct molecular interaction between ICln and OGT confirmed that ICln is O-GlcNAc modified. Mutation of Ser67 destabilized the interaction, suggesting that this amino acid comes in close contact with OGT (Figure 11). Substitution of Ser67 with an Ala should have minimal impact on protein conformation, as the expression levels and activity of ICln Ser67Ala are very similar to that of the wild-type protein (Figures 8A,D). Therefore, alterations in interaction with OGT and insensitivity of the ICln Ser67Ala-induced current to O-GlcNAc are unlikely linked to a variation in protein folding or stability and most likely reflect an impaired O-GlcNAcylation following substitution of Ser67.

Intriguingly, Ser67 lies in close proximity with the amino acid sequence (61)ISLHA(65), which binds the motif KXGFFKR of the intracellular domain of α -integrin as an essential step in IClswell activation (Schedlbauer et al., 2019). This observation prompted us to investigate whether O-GlcNAcylation controls the binding of ICln to integrin α Ib. Surprisingly, the FRET efficiency between the non-glycosylatable ICln Ser67Ala and integrin α Ib was approximately thrice that of the wild-type ICln, thus implying a strong interaction (Figure 12A). This finding suggests that O-GlcNAcylation prevents the interaction between wild-type ICln and α -integrin and further confirms that wild-type ICln is, at least in part, constitutively O-GlcNAcylated. While an increase in the O-GlcNAcylation of cellular proteins significantly reduced the direct molecular interaction between wild-type ICln and α Ib, it did not affect ICln Ser67Ala (Figure 12C). In parallel, a decrease in the O-GlcNAcylation of cellular proteins significantly increased the interaction between wild-type ICln and α Ib, but did not affect ICln Ser67Ala (Figure 12D). The unresponsiveness of the interaction between ICln Ser67Ala and α -integrin to changes in the O-GlcNAcylation levels reflects the insensitivity of the ICln Ser67Ala-induced current to the same conditions (Figure 10). Altogether, these results show that increases in the O-GlcNAcylation of cellular proteins affect RVD by inhibiting

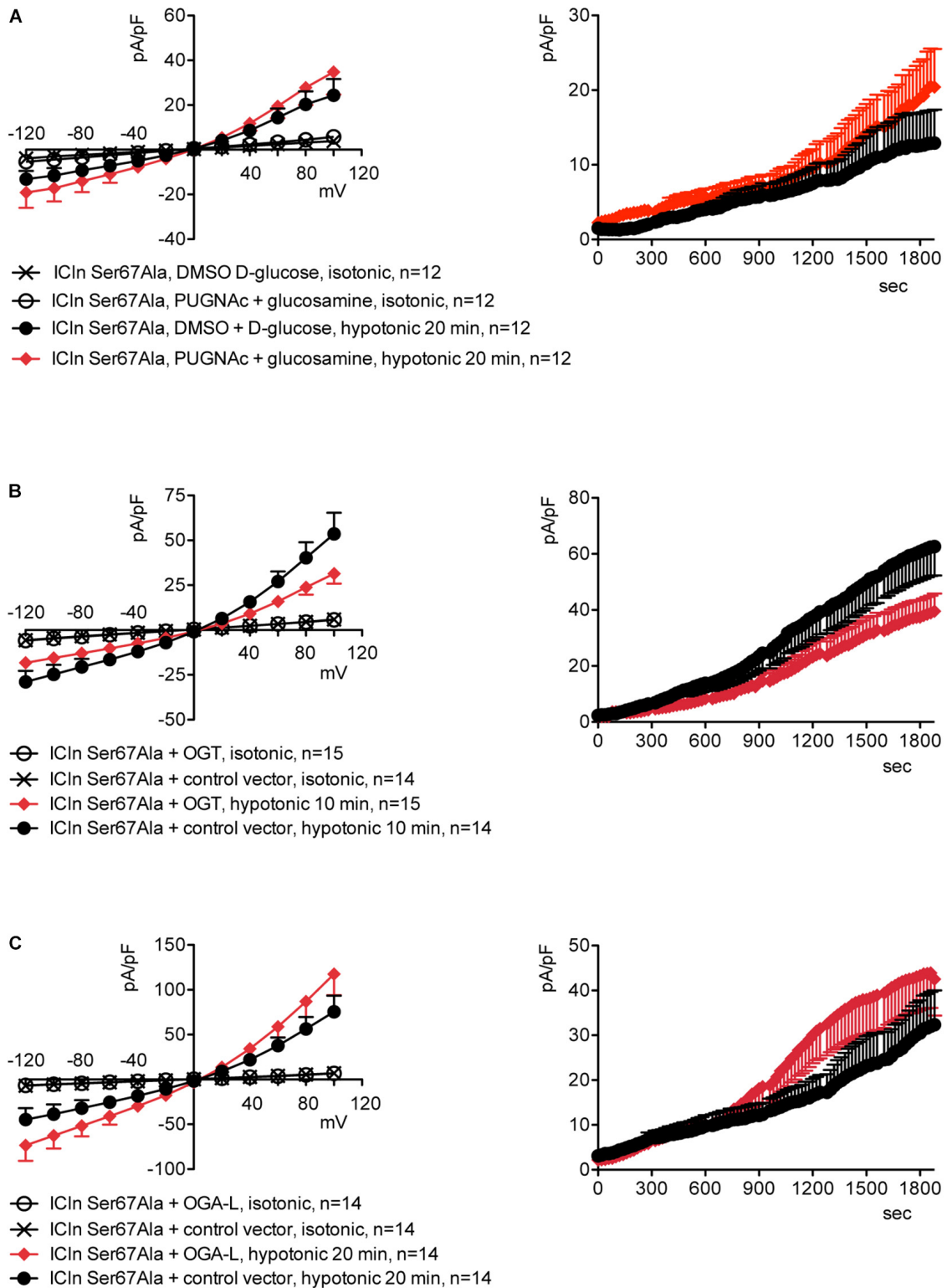
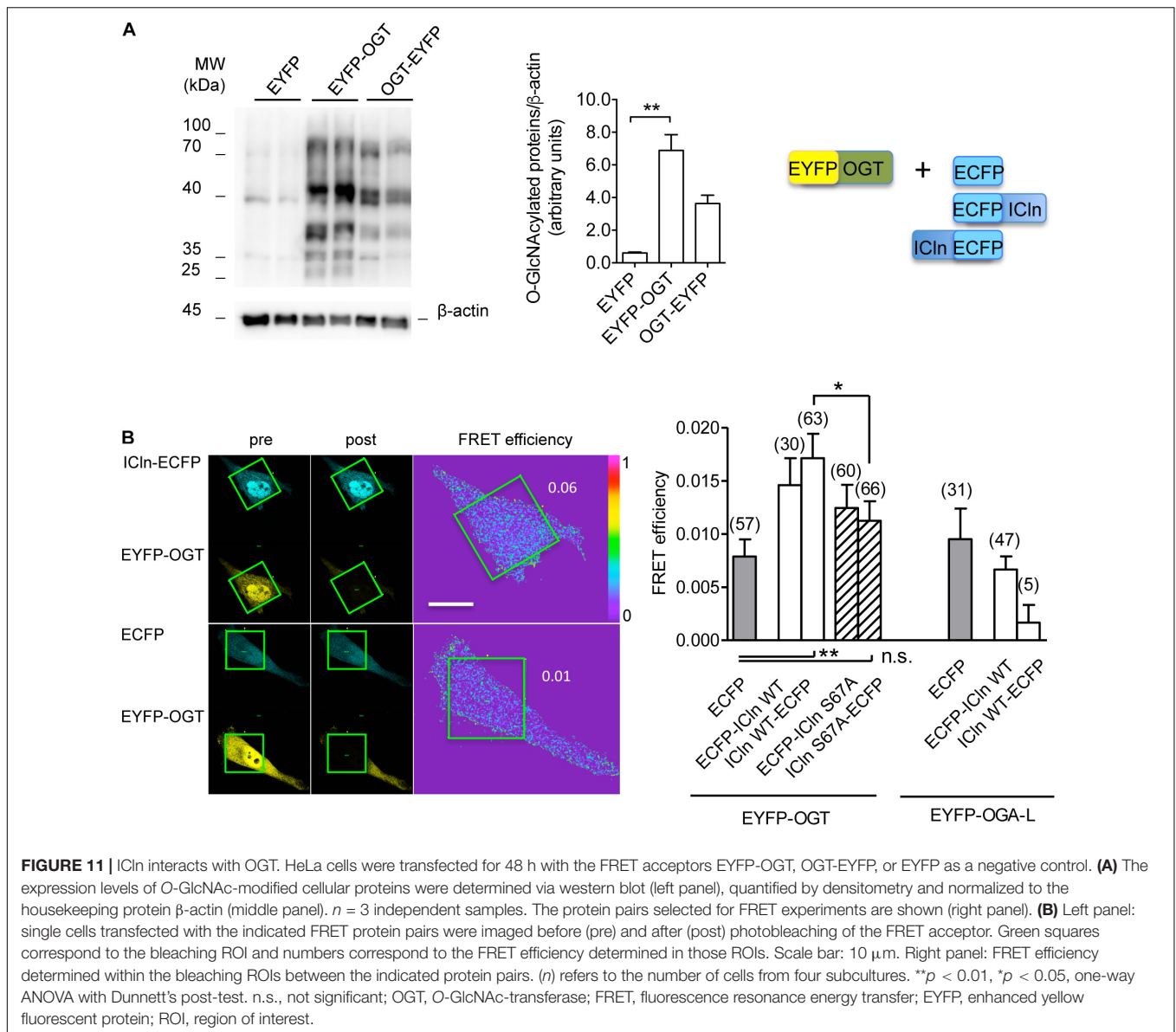


FIGURE 10 | The ICln Ser67Ala-induced ICIswell is unresponsive to variations in O-glycosylation of cellular proteins. ICIswell activation was monitored in HEK 293 Phoenix cells transfected for 24 h with ICln Ser67Ala and the transfection marker dsRed as separate proteins and **(A)** pre-incubated for 1 h with 100 μ M PUGNac plus 5 mM glucosamine or 0.1% DMSO plus 5 mM D-glucose as the control or **(B)** co-transfected with OGT or **(C)** OGA-L and the transfection marker EGFP. The current density-to-voltage relationships determined in an extracellular hypotonic solution (left panels) and the current density-to-time relationships (right panels) of ICIswell are shown. (n) refers to the number of cells. DMSO, dimethyl sulfoxide; EGFP, enhanced green fluorescent protein. OGT, O-GlcNAc transferase; OGA, O-GlcNAcase.



IClswell; IClswell inhibition may derive from O-GlcNAcylation of the protein ICln, with consequent loss of function due to destabilization of the interaction with α-integrin; Ser67 controls the ICln binding to integrin by conferring responsiveness of this interaction to O-GlcNAcylation, thus indicating that this or another amino acid located in close proximity most likely represent an O-GlcNAcylation site.

An increase in the extracellular osmolarity resulted in an increase in the O-GlcNAcylation levels of cellular proteins in mouse embryonic fibroblasts (Zachara et al., 2004), while exposure of HEK293T cells and primary mouse cortical neurons to a hypotonic medium decreased O-GlcNAcylation, as a result of a decline in OGT expression (Kommaddi et al., 2011). Accordingly, we found that exposure of HeLa cells to hypotonicity significantly reduced cellular O-GlcNAcylation abundance (Figure 13). This event would permit an activation

of ICln and, hence, IClswell and RVD, following hypotonic stress. As detailed above, several points of evidence indicate that, in the absence of hypotonic stress, ICln is kept inactive by constitutive O-GlcNAcylation. This concept is further supported by the existence of a significant FRET between ICln and OGT in an isotonic environment, while an interaction with OGA could not be detected in the same condition (Figure 11). Altogether, our findings indicate that hypotonicity would lead to IClswell activation via reduction of ICln O-GlcNAcylation at Ser67, which would permit its direct binding to α-integrin through the neighboring (61)ISLHA(65) motif.

The amino acid sequence (61)ISLHA(65) appears to be crucial in controlling the interaction between ICln and its molecular partners. As multifunctional protein and connector hub, ICln exerts multiple roles within distinct functional modules by interacting with heterogeneous protein targets

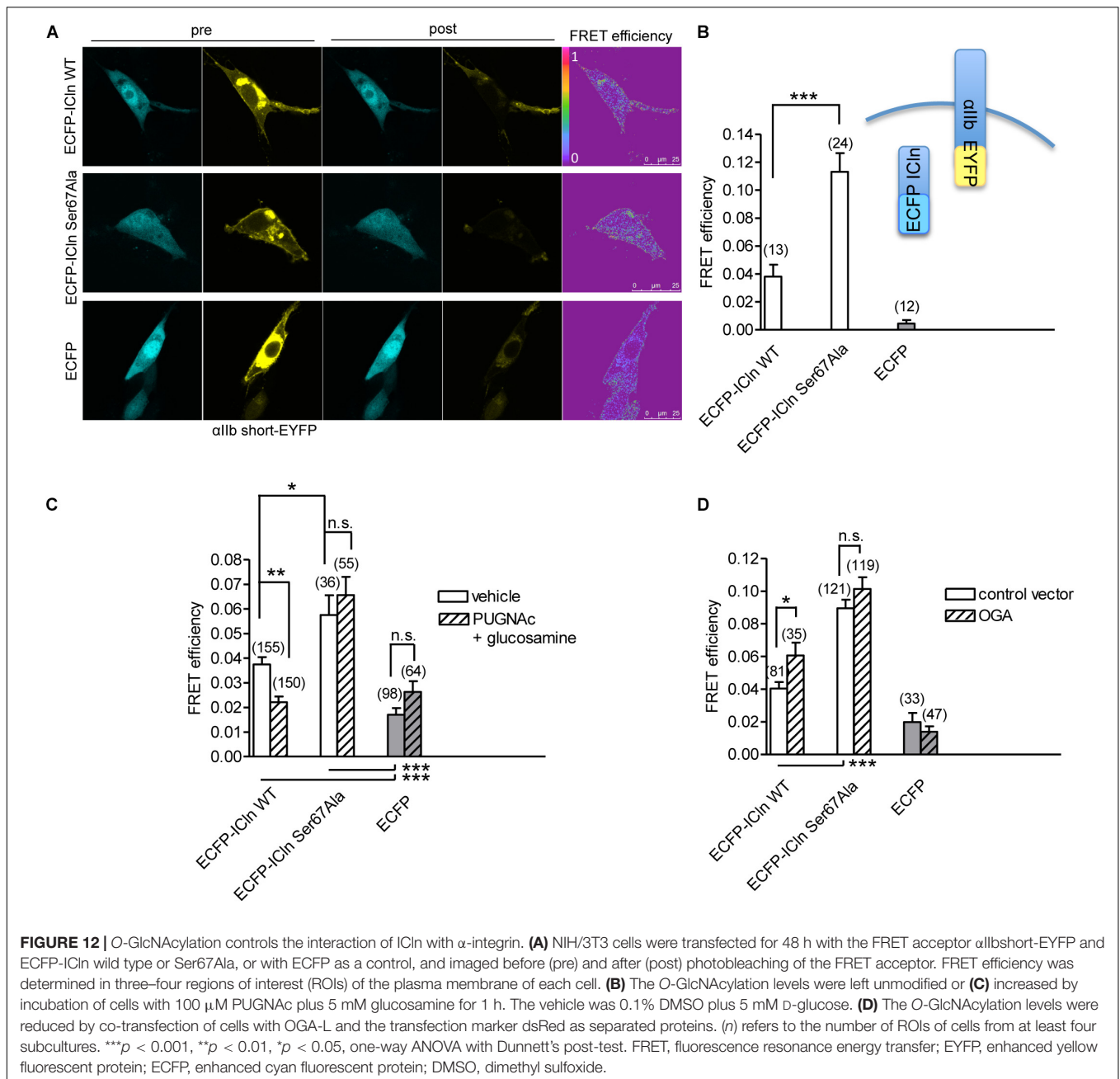
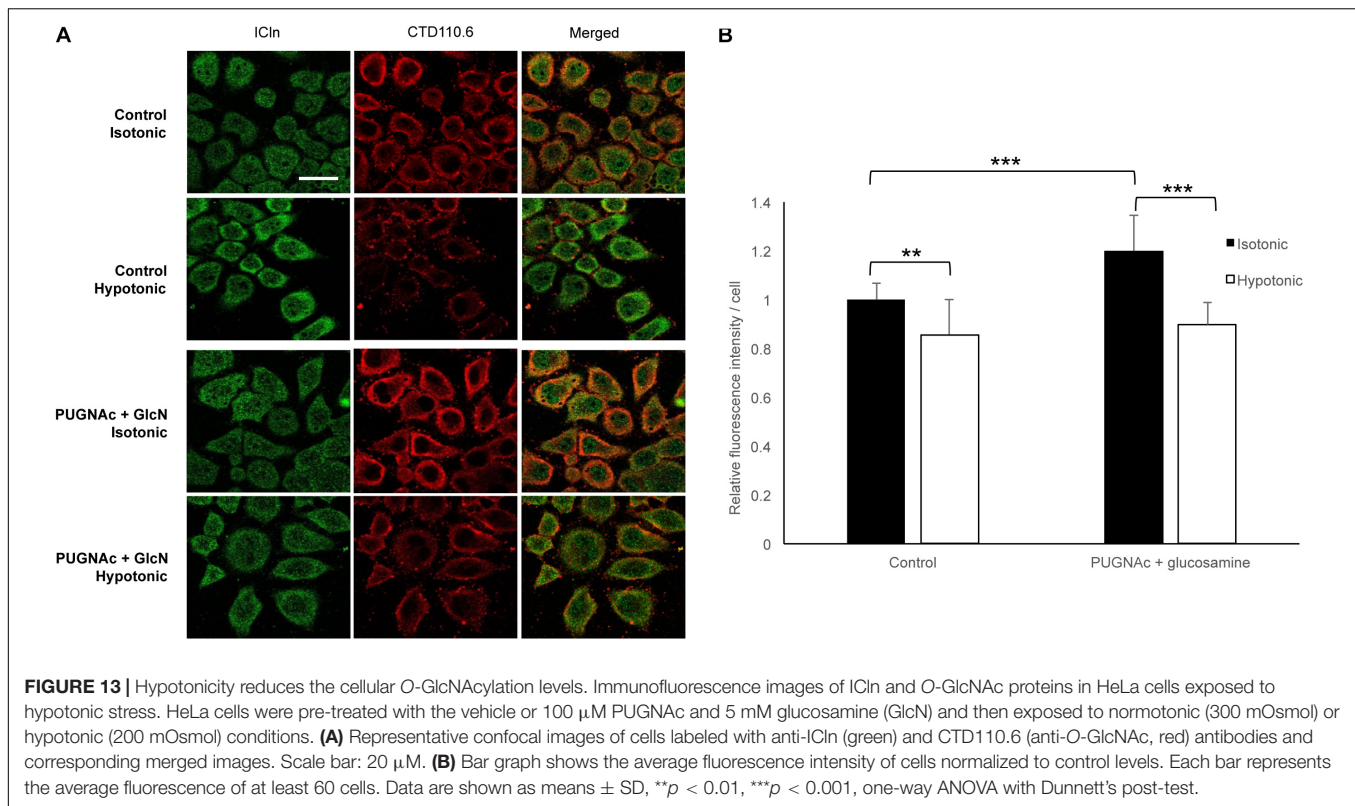


FIGURE 12 | O-GlcNAcylation controls the interaction of ICln with α -integrin. **(A)** NIH/3T3 cells were transfected for 48 h with the FRET acceptor α IIbshort-EYFP and ECFP-ICln wild type or Ser67Ala, or with ECFP as a control, and imaged before (pre) and after (post) photobleaching of the FRET acceptor. FRET efficiency was determined in three–four regions of interest (ROIs) of the plasma membrane of each cell. **(B)** The O-GlcNAcylation levels were left unmodified or **(C)** increased by incubation of cells with 100 μ M PUGNAc plus 5 mM glucosamine for 1 h. The vehicle was 0.1% DMSO plus 5 mM D-glucose. **(D)** The O-GlcNAcylation levels were reduced by co-transfection of cells with OGA-L and the transfection marker dsRed as separated proteins. (n) refers to the number of ROIs of cells from at least four subcultures. *** p < 0.001, ** p < 0.01, * p < 0.05, one-way ANOVA with Dunnett's post-test. FRET, fluorescence resonance energy transfer; EYFP, enhanced yellow fluorescent protein; ECFP, enhanced cyan fluorescent protein; DMSO, dimethyl sulfoxide.

(Furst et al., 2006). In addition to its function in the regulation of cellular volume, ICln acts as an assembly chaperone and Smith antigen (Sm) protein mimic and enables the assembly of the 6S core of the small nuclear ribonucleoproteins (snRNP), which are a key component of the spliceosome (Grimm et al., 2013). Within the ring structure of the 6S complex, ICln establishes a direct molecular interaction with SmD1 and SmG. The ICln–SmD1 interaction interface is centered on the antiparallel β -strand pair represented by the SmD1 β 4 and the ICln β 5. This interaction involves the formation of five backbone–backbone H-bonds involving the residues (61)ISLHA(65) of ICln. A sixth H-bond is formed

between the side-chain hydroxyl group of ICln Ser67 and the backbone carbonyl of SmD1 Gln54. Therefore, it is likely that O-GlcNAcylation of Ser67 also affects the interaction between ICln and SmD1.

In line with our findings, other studies have shown that RVD and IClswell magnitude were reduced in mouse models of diabetes mellitus, a condition where O-GlcNAc is chronically elevated. For example, in white adipocytes isolated from yellow Kuo Kondo (KKA^y) diabetic mice, RVD rate and IClswell magnitude were lower than those measured in adipocytes of normal C57BL/6 or KK mice, a parental strain of KKA^y mice that do not manifest diabetes until an older age (Inoue et al., 2010).



Accordingly, RVD was almost lost and IClswell magnitude was significantly reduced in ventricular myocytes of streptozotocin-induced mice, a well-established model of type 1 diabetes (Yamamoto et al., 2009). Importantly, the RVD rate was heavily reduced also in platelets derived from diabetic patients (Margalit et al., 1995). However, the cellular O-GlcNAc levels in these three latter studies were not measured, and the possible link between increased O-GlcNAc and impaired RVD was not assessed.

As already mentioned, O-GlcNAc modification is involved in the development of insulin resistance and chronic complications of diabetes mellitus (Vaidyanathan and Wells, 2014; Peterson and Hart, 2016), which could in principle be correlated to an impairment of RVD and/or IClswell. Diabetic nephropathy is a clinical syndrome characterized by kidney damage and may result in renal failure (Sun et al., 2013). The cellular and molecular mechanisms leading to diabetic nephropathy are complex and only partially understood. Although the glomerulus has historically been considered as the primary site of diabetic kidney injury, it is becoming increasingly evident that hyperglycemia-induced tubular lesions are prominent components of diabetic nephropathy (Bagby, 2007; Tang and Lai, 2012). The kidney plays the crucial function of controlling the systemic blood pressure and electrolyte balance and is often subjected to osmotic stress during the phenomena of diuresis and anti-diuresis. In addition, in diabetes mellitus, high levels of glucose in the glomerular filtrate lead to an increased reabsorption of glucose and sodium by SGLT2 and SGLT1 in the proximal tubule, along with passive reabsorption of chloride

and water (Vallon and Thomson, 2020). It is well known that cells in absorptive epithelia need to efficiently regulate their volume following increases in the intracellular concentration of osmo-active substances, including glucose (van der Wijk et al., 2000). Therefore, although pathological changes like renal fibrosis, mesangial expansion, glomerular hypertrophy, inflammation, and oxidative stress seem to be the main events leading to diabetic nephropathy (Bhattacharjee et al., 2016), we suggest that an impaired or insufficient RVD of kidney tubular cells, which leads to necrotic cell death (Okada et al., 2001, 2019), may contribute to the development of kidney damage in the context of uncontrolled or poorly controlled diabetes mellitus.

Former studies exploring the role of O-GlcNAc in diabetic nephropathy mimicked hyperglycemic conditions by exposing various cell types to 20–35 mM D-glucose for 24–48 h (Park et al., 2014; Eleftheriadis et al., 2016, 2020; Gellai et al., 2016). The relatively short incubation time used in the present work (1 h) aimed at disclosing early pathophysiological changes prior overt derangements of cell homeostatic functions occurred. HEK 293 cells, which originate from embryonic kidney, are probably largely undifferentiated but show characteristics of renal epithelial cells and express markers of the proximal tubule, such as SGLT1 (Kaji et al., 2018). HEK 293 cells behavior did not significantly differ from that of HK2 cells—an immortalized proximal tubule epithelial cell line, in an *in vitro* model of diabetic nephropathy (Masola et al., 2011). Other cells used in the present work were chosen as a convenient overexpression system of ectopic proteins. It would be important to confirm the findings

presented here, and especially a GlcNAc-induced alteration in RVD, in better models of kidney tubular cells, such as primary human renal proximal tubular epithelial cells.

ICln interacts with multiple partner proteins to participate in multiple cellular functions (Furst et al., 2006). It is tempting to speculate that phosphorylation of Thr223 and/or O-GlcNAc modification of the C-terminus of ICln might control its interactome. Further studies are needed to explore this hypothesis.

In conclusion, an increased O-GlcNAcylation of cellular proteins leads to impairment of the homeostatic reaction of RVD by suppressing the swelling-activated chloride current IC_{swell}. IC_{swell} suppression is linked to an inhibition of function of the protein ICln subsequent to O-GlcNAcylation at Ser67, which leads to destabilization of its direct interaction with the intracellular domain of α -integrin. These results underscore the essential role of O-GlcNAc modification in governing basic cell homeostatic functions by controlling protein–protein interactions, and further suggest that reducing ICln O-GlcNAcylation may represent a novel strategy in the prevention or treatment of diseases where an RVD derangement might be involved, including chronic complications of diabetes mellitus such as diabetic nephropathy.

DATA AVAILABILITY STATEMENT

The original contributions presented in the study are included in the article/**Supplementary Material**, further inquiries can be directed to the corresponding author. The mass spectrometry proteomics data from this study were deposited in the ProteomeXchange Consortium via the jPOST (Okuda et al.,

2017) partner repository with the dataset identifier PXD022389 and doi: 10.6019/PXD022389.

AUTHOR CONTRIBUTIONS

TN, MP, and SD conceived the study. TN, SD, MP, WP, AS, TJ, AMi, RM, and AMa designed the experiments and interpreted the results. RC, AR, DAC, EB, ZS, TN, and SD performed the experiments and analyzed the data. MP, AMi, AMa, WP, and TJ acquired funding. SD wrote the original draft. WP edited and all authors reviewed and approved the final version of the manuscript.

FUNDING

AR was supported by the Programma Operativo Nazionale (PON) Ricerca e Innovazione, “Dottorati Innovativi con caratterizzazione Industriale” 2014–2020, Fondo Sociale Europeo fellowship. DC was supported by the Harvard/Salzburg-Stipendium 02/00/28060/2013/064 (Stadt Salzburg).

ACKNOWLEDGMENTS

The authors acknowledge the expert secretarial assistance of Elisabeth Mooslechner.

SUPPLEMENTARY MATERIAL

The Supplementary Material for this article can be found online at: <https://www.frontiersin.org/articles/10.3389/fcell.2020.607080/full#supplementary-material>

REFERENCES

- Bagby, S. P. (2007). Diabetic nephropathy and proximal tubule ROS: challenging our glomerulocentricity. *Kidney Int.* 71, 1199–1202. doi: 10.1038/sj.ki.5002286
- Banerjee, P. S., Lagerlof, O., and Hart, G. W. (2016). Roles of O-GlcNAc in chronic diseases of aging. *Mol. Aspects Med.* 51, 1–15. doi: 10.1016/j.mam.2016.05.005
- Bhattacharjee, N., Barma, S., Konwar, N., Dewanjee, S., and Manna, P. (2016). Mechanistic insight of diabetic nephropathy and its pharmacotherapeutic targets: an update. *Eur. J. Pharmacol.* 791, 8–24. doi: 10.1016/j.ejphar.2016.08.022
- Blom, N., Sicheritz-Ponten, T., Gupta, R., Gammeltoft, S., and Brunak, S. (2004). Prediction of post-translational glycosylation and phosphorylation of proteins from the amino acid sequence. *Proteomics* 4, 1633–1649. doi: 10.1002/pmic.200300771
- Brownlee, M. (2001). Biochemistry and molecular cell biology of diabetic complications. *Nature* 414, 813–820. doi: 10.1038/414813a
- Buse, M. G. (2006). Hexosamines, insulin resistance, and the complications of diabetes: current status. *Am. J. Physiol. Endocrinol. Metab.* 290, E1–E8. doi: 10.1152/ajpendo.00329.2005
- Butkinaree, C., Park, K., and Hart, G. W. (2010). O-linked beta-N-acetylglucosamine (O-GlcNAc): extensive crosstalk with phosphorylation to regulate signaling and transcription in response to nutrients and stress. *Biochim. Biophys. Acta* 1800, 96–106. doi: 10.1016/j.bbagen.2009.07.018
- Chambers, M. C., Maclean, B., Burke, R., Amodei, D., Ruderman, D. L., Neumann, S., et al. (2012). A cross-platform toolkit for mass spectrometry and proteomics. *Nat. Biotechnol.* 30, 918–920. doi: 10.1038/nbt.2377
- Champattanachai, V., Marchase, R. B., and Chatham, J. C. (2008). Glucosamine protects neonatal cardiomyocytes from ischemia-reperfusion injury via increased protein O-GlcNAc and increased mitochondrial Bcl-2. *Am. J. Physiol. Cell Physiol.* 294, C1509–C1520. doi: 10.1152/ajpcell.00456.2007
- Copeland, R. J., Bullen, J. W., and Hart, G. W. (2008). Cross-talk between GlcNAcylation and phosphorylation: roles in insulin resistance and glucose toxicity. *Am. J. Physiol. Endocrinol. Metab.* 295, E17–E28. doi: 10.1152/ajpendo.90281.2008
- Daxecker, H., Raab, M., Bernard, E., Devocelle, M., Treumann, A., and Moran, N. (2008). A peptide affinity column for the identification of integrin α IIb-binding proteins. *Anal. Biochem.* 374, 203–212. doi: 10.1016/j.ab.2007.11.033
- Dias, W. B., and Hart, G. W. (2007). O-GlcNAc modification in diabetes and Alzheimer's disease. *Mol. Biosyst.* 3, 766–772. doi: 10.1039/b704905f
- DiCiommo, D. P., Duckett, A., Burcescu, I., Bremner, R., and Gallie, B. L. (2004). Retinoblastoma protein purification and transduction of retina and retinoblastoma cells using improved alphavirus vectors. *Invest. Ophthalmol. Vis. Sci.* 45, 3320–3329. doi: 10.1167/iovos.04-0140

- Dossena, S., Gandini, R., Tamma, G., Vezzoli, V., Nofziger, C., Tamplenizza, M., et al. (2011). The molecular and functional interaction between ICln and HSPC038 proteins modulates the regulation of cell volume. *J. Biol. Chem.* 286, 40659–40670. doi: 10.1074/jbc.M111.260430
- Eleftheriadis, T., Pissas, G., Tsogka, K., Nikolaou, E., Liakopoulos, V., and Stefanidis, I. (2020). A unifying model of glucotoxicity in human renal proximal tubular epithelial cells and the effect of the SGLT2 inhibitor dapagliflozin. *Int. Urol. Nephrol.* 52, 1179–1189. doi: 10.1007/s11255-020-02481-3
- Eleftheriadis, T., Tsogka, K., Pissas, G., Antoniadis, G., Liakopoulos, V., and Stefanidis, I. (2016). Activation of general control nonderepressible 2 kinase protects human glomerular endothelial cells from harmful high-glucose-induced molecular pathways. *Int. Urol. Nephrol.* 48, 1731–1739. doi: 10.1007/s11255-016-1377-x
- Fardini, Y., Dehennaut, V., Lefebvre, T., and Issad, T. (2013). O-GlcNAcylation: a new cancer hallmark? *Front. Endocrinol.* 4:99. doi: 10.3389/fendo.2013.00099
- Ferron, M., Denis, M., Persello, A., Rathagirisnan, R., and Lauzier, B. (2018). Protein O-GlcNAcylation in cardiac pathologies: past, present, future. *Front. Endocrinol.* 9:819. doi: 10.3389/fendo.2018.00819
- Fisi, V., Miseta, A., and Nagy, T. (2017). The role of stress-induced O-GlcNAc protein modification in the regulation of membrane transport. *Oxid. Med. Cell Longev.* 2017:1308692. doi: 10.1155/2017/1308692
- Friedrich, B., Matskevich, I., and Lang, F. (2006). Cell volume regulatory mechanisms. *Contrib. Nephrol.* 152, 1–8. doi: 10.1159/000096284
- Furst, J., Botta, G., Saino, S., Dopinto, S., Gandini, R., Dossena, S., et al. (2006). The ICln interactome. *Acta Physiol.* 187, 43–49. doi: 10.1111/j.1748-1716.2006.01549.x
- Furst, J., Gschwentner, M., Ritter, M., Botta, G., Jakab, M., Mayer, M., et al. (2002a). Molecular and functional aspects of anionic channels activated during regulatory volume decrease in mammalian cells. *Pflug. Arch* 444, 1–25. doi: 10.1007/s00424-002-0805-1
- Furst, J., Ritter, M., Rudzki, J., Danzl, J., Gschwentner, M., Scandella, E., et al. (2002b). ICln ion channel splice variants in *Caenorhabditis elegans*: voltage dependence and interaction with an operon partner protein. *J. Biol. Chem.* 277, 4435–4445. doi: 10.1074/jbc.M107372200
- Furst, J., Schedlbauer, A., Gandini, R., Garavaglia, M. L., Saino, S., Gschwentner, M., et al. (2005). ICln159 folds into a pleckstrin homology domain-like structure. Interaction with kinases and the splicing factor LSM4. *J. Biol. Chem.* 280, 31276–31282. doi: 10.1074/jbc.M500541200
- Gandini, R., Dossena, S., Vezzoli, V., Tamplenizza, M., Salvioni, E., Ritter, M., et al. (2008). LSM4 associates with the plasma membrane and acts as a co-factor in cell volume regulation. *Cell Physiol. Biochem.* 22, 579–590. doi: 10.1159/000185542
- Gellai, R., Hodrea, J., Lenart, L., Hosszu, A., Koszegi, S., Balogh, D., et al. (2016). Role of O-linked N-acetylglucosamine modification in diabetic nephropathy. *Am. J. Physiol. Renal Physiol.* 311, F1172–F1181. doi: 10.1152/ajprenal.00545.2015
- Gloster, T. M., and Vocadlo, D. J. (2010). Mechanism, structure, and inhibition of O-GlcNAc processing enzymes. *Curr. Signal Transduct. Ther.* 5, 74–91. doi: 10.2174/157436210790226537
- Grimm, C., Chari, A., Pelz, J. P., Kuper, J., Kisker, C., Diederichs, K., et al. (2013). Structural basis of assembly chaperone-mediated snRNP formation. *Mol. Cell* 49, 692–703. doi: 10.1016/j.molcel.2012.12.009
- Gupta, R., and Brunak, S. (2002). Prediction of glycosylation across the human proteome and the correlation to protein function. *Pac. Symp. Biocomput.* 2002, 310–322.
- Hahne, H., Sobotzki, N., Nyberg, T., Helm, D., Borodkin, V. S., van Aalten, D. M., et al. (2013). Proteome wide purification and identification of O-GlcNAc-modified proteins using click chemistry and mass spectrometry. *J. Prot. Res.* 12, 927–936. doi: 10.1021/pr300967y
- Hart, G. W. (2014). Three Decades of Research on O-GlcNAcylation - a major nutrient sensor that regulates signaling, transcription and cellular metabolism. *Front. Endocrinol.* 5:183. doi: 10.3389/fendo.2014.00183
- Hart, G. W. (2019). Nutrient regulation of signaling and transcription. *J. Biol. Chem.* 294, 2211–2231. doi: 10.1074/jbc.AW119.003226
- Hart, G. W., Housley, M. P., and Slawson, C. (2007). Cycling of O-linked beta-N-acetylglucosamine on nucleocytoplasmic proteins. *Nature* 446, 1017–1022. doi: 10.1038/nature05815
- Hart, G. W., Slawson, C., Ramirez-Correa, G., and Lagerlof, O. (2011). Cross talk between O-GlcNAcylation and phosphorylation: roles in signaling, transcription, and chronic disease. *Annu. Rev. Biochem.* 80, 825–858. doi: 10.1146/annurev-biochem-060608-102511
- Hoffmann, E. K., Lambert, I. H., and Pedersen, S. F. (2009). Physiology of cell volume regulation in vertebrates. *Physiol. Rev.* 89, 193–277. doi: 10.1152/physrev.00037.2007
- Hubert, M. D., Levitan, I., Hoffman, M. M., Zraggen, M., Hofreiter, M. E., and Garber, S. S. (2000). Modulation of volume regulated anion current by I(Cln). *Biochim. Biophys. Acta* 1466, 105–114. doi: 10.1016/S0005-2736(00)00177-2
- Inoue, H., Takahashi, N., Okada, Y., and Konishi, M. (2010). Volume-sensitive outwardly rectifying chloride channel in white adipocytes from normal and diabetic mice. *Am. J. Physiol. Cell Physiol.* 298, C900–C909. doi: 10.1152/ajpcell.00450.2009
- Jakab, M., Furst, J., Gschwentner, M., Botta, G., Garavaglia, M. L., Bazzini, C., et al. (2002). Mechanisms sensing and modulating signals arising from cell swelling. *Cell Physiol. Biochem.* 12, 235–258. doi: 10.1159/000067895
- Jia, C., and Zuo, Y. (2018). Computational Prediction of Protein O-GlcNAc Modification. *Methods Mol. Biol.* 1754, 235–246. doi: 10.1007/978-1-4939-7717-8_14
- Kaji, K., Nishimura, N., Seki, K., Sato, S., Saikawa, S., Nakanishi, K., et al. (2018). Sodium glucose cotransporter 2 inhibitor canagliflozin attenuates liver cancer cell growth and angiogenic activity by inhibiting glucose uptake. *Int. J. Cancer* 142, 1712–1722. doi: 10.1002/ijc.31193
- Kim, E. J., Kang, D. O., Love, D. C., and Hanover, J. A. (2006). Enzymatic characterization of O-GlcNAcase isoforms using a fluorogenic GlcNAc substrate. *Carbohydr. Res.* 341, 971–982. doi: 10.1016/j.carres.2006.03.004
- Kneass, Z. T., and Marchase, R. B. (2004). Neutrophils exhibit rapid agonist-induced increases in protein-associated O-GlcNAc. *J. Biol. Chem.* 279, 45759–45765. doi: 10.1074/jbc.M407911200
- Kommaddi, R. P., Dickson, K. M., and Barker, P. A. (2011). Stress-induced expression of the p75 neurotrophin receptor is regulated by O-GlcNAcylation of the Sp1 transcription factor. *J. Neurochem.* 116, 396–405. doi: 10.1111/j.1471-4159.2010.07120.x
- Lagerlof, O., and Hart, G. W. (2014). O-GlcNAcylation of neuronal proteins: roles in neuronal functions and in neurodegeneration. *Adv. Neurobiol.* 9, 343–366. doi: 10.1007/978-1-4939-1154-7_16
- Lang, F., Bush, G. L., Ritter, M., Völkl, H., Waldegger, S., Gulbins, E., et al. (1998). Functional significance of cell volume regulatory mechanisms. *Physiol. Rev.* 78, 247–306. doi: 10.1152/physrev.1998.78.1.247
- Larkin, D., Murphy, D., Reilly, D. F., Cahill, M., Sattler, E., Harriott, P., et al. (2004). ICln, a novel integrin alphaIIb beta3-associated protein, functionally regulates platelet activation. *J. Biol. Chem.* 279, 27286–27293. doi: 10.1074/jbc.M402159200
- Larkin, D., Treumann, A., Murphy, D., DeChaumont, C., Kiernan, A., and Moran, N. (2009). Compartmentalization regulates the interaction between the platelet integrin alpha IIb beta 3 and ICln. *Br. J. Haematol.* 144, 580–590. doi: 10.1111/j.1365-2141.2008.07483.x
- Li, F., Li, C., Wang, M., Webb, G. I., Zhang, Y., Whisstock, J. C., et al. (2015). GlycoMine: a machine learning-based approach for predicting N-, C- and O-linked glycosylation in the human proteome. *Bioinformatics* 31, 1411–1419. doi: 10.1093/bioinformatics/btu852
- Liu, Y., Zhang, H., Men, H., Du, Y., Xiao, Z., Zhang, F., et al. (2019). Volume-regulated Cl(-) current: contributions of distinct Cl(-) channels and localized Ca(2+) signals. *Am. J. Physiol. Cell Physiol.* 317, C466–C480. doi: 10.1152/ajpcell.00507.2018
- Ma, J., and Hart, G. W. (2014). O-GlcNAc profiling: from proteins to proteomes. *Clin. Prot.* 11:8. doi: 10.1186/1559-0275-11-8
- Margalit, A., Gilutz, H., and Granot, Y. (1995). Original article: low regulatory volume decrease rate in platelets from ischemic patients: a possible role

- for heparanase in thrombogenicity. *Platelets* 6, 371–376. doi: 10.3109/09537109509078474
- Masola, V., Gambaro, G., Tibaldi, E., Onisto, M., Abaterusso, C., and Lupo, A. (2011). Regulation of heparanase by albumin and advanced glycation end products in proximal tubular cells. *Biochim. Biophys. Acta* 1813, 1475–1482. doi: 10.1016/j.bbamer.2011.05.004
- McClain, D. A., and Crook, E. D. (1996). Hexosamines and insulin resistance. *Diabetes* 45, 1003–1009. doi: 10.2337/diab.45.8.1003
- McLarty, J. L., Marsh, S. A., and Chatham, J. C. (2013). Post-translational protein modification by O-linked N-acetyl-glucosamine: its role in mediating the adverse effects of diabetes on the heart. *Life Sci.* 92, 621–627. doi: 10.1016/j.lfs.2012.08.006
- Morabito, R., Costa, R., Rizzo, V., Remigante, A., Nofziger, C., La Spada, G., et al. (2017). Crude venom from nematocysts of *Pelagia noctiluca* (Cnidaria: Scyphozoa) elicits a sodium conductance in the plasma membrane of mammalian cells. *Sci. Rep.* 7:41065. doi: 10.1038/srep41065
- Morabito, R., La Spada, G., Dossena, S., and Marino, A. (2014). Oxidative stress affects responsiveness to hypotonicity of renal cells. *J. Biol. Res.* 87:4811.
- Morabito, R., Marino, A., Lauf, P. K., Adragna, N. C., and La Spada, G. (2013). Sea water acidification affects osmotic swelling, regulatory volume decrease and discharge in nematocytes of the jellyfish *Pelagia noctiluca*. *Cell Physiol. Biochem.* 32, 77–85. doi: 10.1159/000356629
- Morgan, R. A., Couture, L., Elroy-Stein, O., Ragheb, J., Moss, B., and Anderson, W. F. (1992). Retroviral vectors containing putative internal ribosome entry sites: development of a polycistronic gene transfer system and applications to human gene therapy. *Nucl. Acids Res.* 20, 1293–1299. doi: 10.1093/nar/20.6.1293
- Myslicki, J. P., Shearer, J., Hittel, D. S., Hughey, C. C., and Belke, D. D. (2014). O-GlcNAc modification is associated with insulin sensitivity in the whole blood of healthy young adult males. *Diabetol. Metab. Syndr.* 6:96. doi: 10.1186/1758-5996-6-96
- Nagy, T., Balasa, A., Frank, D., Rab, A., Rideg, O., Kotek, G., et al. (2010). O-GlcNAc modification of proteins affects volume regulation in Jurkat cells. *Eur. Biophys. J.* 39, 1207–1217. doi: 10.1007/s00249-009-0573-3
- Nagy, T., Miseta, A., and Kovacs, G. L. (2007). Protein-associated O-GlcNAc, a multifunctional mechanism in cell signaling and its role in the pathogenesis of diabetes, stress and malignant diseases. *Biochem. Medica* 17, 162–177. doi: 10.11613/bm.2007.015
- Okada, Y., Maeno, E., Shimizu, T., Dezaki, K., Wang, J., and Morishima, S. (2001). Receptor-mediated control of regulatory volume decrease (RVD) and apoptotic volume decrease (AVD). *J. Physiol.* 532(Pt. 1), 3–16. doi: 10.1111/j.1469-7793.2001.0003g.x
- Okada, Y., Numata, T., Sato-Numata, K., Sabirov, R. Z., Liu, H., Mori, S. I., et al. (2019). Roles of volume-regulatory anion channels, VSOR and Maxi-Cl, in apoptosis, cisplatin resistance, necrosis, ischemic cell death, stroke and myocardial infarction. *Curr. Top. Membr.* 83, 205–283. doi: 10.1016/bs.ctm.2019.03.001
- Okuda, S., Watanabe, Y., Moriya, Y., Kawano, S., Yamamoto, T., Matsumoto, M. et al. (2017). jPOSTrepo: an international standard data repository for proteomes. *Nucl. Acids Res.* 45, D1107–D1111. doi: 10.1093/nar/gkw1080
- Pagesy, P., Tachet, C., Mostefa-Kara, A., Larger, E., and Issad, T. (2018). Increased OGA expression and activity in leukocytes from patients with diabetes: correlation with inflammation markers. *Exp. Clin. Endocrinol. Diabetes* 127, 517–523. doi: 10.1055/a-0596-7337
- Park, K., Saudek, C. D., and Hart, G. W. (2010). Increased expression of beta-N-acetylglucosaminidase in erythrocytes from individuals with pre-diabetes and diabetes. *Diabetes* 59, 1845–1850. doi: 10.2337/db09-1086
- Park, M. J., Kim, D. I., Lim, S. K., Choi, J. H., Han, H. J., Yoon, K. C., et al. (2014). High glucose-induced O-GlcNAcylated carbohydrate response element-binding protein (ChREBP) mediates mesangial cell lipogenesis and fibrosis: the possible role in the development of diabetic nephropathy. *J. Biol. Chem.* 289, 13519–13530. doi: 10.1074/jbc.M113.530139
- Paulmichl, M., Li, Y., Wickman, K., Ackerman, M., Peralta, E., and Clapham, D. (1992). New mammalian chloride channel identified by expression cloning. *Nature* 356, 238–241. doi: 10.1038/356238a0
- Pedersen, S. F., Okada, Y., and Nilius, B. (2016). Biophysics and physiology of the volume-regulated anion channel (VRAC)/volume-sensitive outwardly rectifying anion channel (VSOR). *Pflug. Arch.* 468, 371–383. doi: 10.1007/s00424-015-1781-6
- Peterson, S. B., and Hart, G. W. (2016). New insights: a role for O-GlcNAcylation in diabetic complications. *Crit. Rev. Biochem. Mol. Biol.* 51, 150–161. doi: 10.3109/10409238.2015.1135102
- Qiu, Z., Dubin, A. E., Mathur, J., Tu, B., Reddy, K., Miraglia, L. J., et al. (2014). SWELL1, a plasma membrane protein, is an essential component of volume-regulated anion channel. *Cell* 157, 447–458. doi: 10.1016/j.cell.2014.03.024
- Ritter, M., Ravasio, A., Jakab, M., Chwatal, S., Furst, J., Laich, A., et al. (2003). Cell swelling stimulates cytosol to membrane transposition of ICl_n. *J. Biol. Chem.* 278, 50163–50174. doi: 10.1074/jbc.M300374200
- Schedlbauer, A., Tamma, G., Rodighiero, S., Civello, D. A., Tamplenizza, M., Ledolter, K., et al. (2019). Binding of the protein ICl_n to alpha-integrin contributes to the activation of ICl_nswell current. *Sci. Rep.* 9:12195. doi: 10.1038/s41598-019-48496-4
- Slawson, C., and Hart, G. W. (2011). O-GlcNAc signalling: implications for cancer cell biology. *Nat. Rev. Cancer* 11, 678–684. doi: 10.1038/nrc3114
- Springhorn, C., Matsha, T. E., Erasmus, R. T., and Essop, M. F. (2012). Exploring leukocyte O-GlcNAcylation as a novel diagnostic tool for the earlier detection of type 2 diabetes mellitus. *J. Clin. Endocrinol. Metab.* 97, 4640–4649. doi: 10.1210/jc.2012-2229
- Stowell, S. R., Ju, T., and Cummings, R. D. (2015). Protein glycosylation in cancer. *Annu. Rev. Pathol.* 10, 473–510. doi: 10.1146/annurev-pathol-012414-040438
- Sun, Y. M., Su, Y., Li, J., and Wang, L. F. (2013). Recent advances in understanding the biochemical and molecular mechanism of diabetic nephropathy. *Biochem. Biophys. Res. Commun.* 433, 359–361. doi: 10.1016/j.bbrc.2013.02.120
- Szabo, Z., Szomor, J. S., Foeldi, I., and Janaky, T. (2012). Mass spectrometry-based label free quantification of gel separated proteins. *J. Proteomics* 75, 5544–5553. doi: 10.1016/j.jpro.2012.07.036
- Tamma, G., Dossena, S., Nofziger, C., Valenti, G., Svelto, M., and Paulmichl, M. (2011). EGF stimulates ICl_nswell by a redistribution of proteins involved in cell volume regulation. *Cell Physiol. Biochem.* 28, 1191–1202. doi: 10.1159/000355851
- Tang, S. C., and Lai, K. N. (2012). The pathogenic role of the renal proximal tubular cell in diabetic nephropathy. *Nephrol. Dial. Transpl.* 27, 3049–3056. doi: 10.1093/ndt/gfs260
- Vaidyanathan, K., and Wells, L. (2014). Multiple tissue-specific roles for the O-GlcNAc post-translational modification in the induction of and complications arising from type II diabetes. *J. Biol. Chem.* 289, 34466–34471. doi: 10.1074/jbc.R114.591560
- Vallon, V., and Thomson, S. C. (2020). The tubular hypothesis of nephron filtration and diabetic kidney disease. *Nat. Rev. Nephrol.* 16, 317–336. doi: 10.1038/s41581-020-0256-y
- van der Wijk, T., Tomassen, S. F., de Jonge, H. R., and Tilly, B. C. (2000). Signalling mechanisms involved in volume regulation of intestinal epithelial cells. *Cell Physiol. Biochem.* 10, 289–296. doi: 10.1159/000016359
- Vaudel, M., Burkhardt, J. M., Zahedi, R. P., Oveland, E., Berven, F. S., Sickmann, A., et al. (2015). PeptideShaker enables reanalysis of MS-derived proteomics data sets. *Nat. Biotechnol.* 33, 22–24. doi: 10.1038/nbt.3109
- Voss, F. K., Ullrich, F., Munch, J., Lazarow, K., Lutter, D., Mah, N., et al. (2014). Identification of LRRC8 heteromers as an essential component of the volume-regulated anion channel VRAC. *Science* 344, 634–638. doi: 10.1126/science.1252826
- Wang, S., Yang, F., Camp, D. G. II, Rodland, K., Qian, W. J., Liu, T., et al. (2014). Proteomic approaches for site-specific O-GlcNAcylation analysis. *Bioanalysis* 6, 2571–2580. doi: 10.4155/bio.14.239
- Wang, Z., Park, K., Comer, F., Hsieh-Wilson, L. C., Saudek, C. D., and Hart, G. W. (2009). Site-specific GlcNAcylation of human erythrocyte proteins: potential biomarker(s) for diabetes. *Diabetes* 58, 309–317. doi: 10.2337/db08-0994
- Wells, L., Vosseller, K., and Hart, G. W. (2001). Glycosylation of nucleocytoplasmic proteins: signal transduction and O-GlcNAc. *Science* 291, 2376–2378. doi: 10.1126/science.1058714
- Wells, L., Vosseller, K., and Hart, G. W. (2003a). A role for N-acetylglucosamine as a nutrient sensor and mediator of insulin resistance. *Cell Mol. Life Sci.* 60, 222–228. doi: 10.1007/s000180300017
- Wells, L., Whelan, S. A., and Hart, G. W. (2003b). O-GlcNAc: a regulatory post-translational modification. *Biochem. Biophys. Res. Commun.* 302, 435–441. doi: 10.1016/s0006-291x(03)00175-x

- Yamamoto, S., Ichishima, K., and Ehara, T. (2009). Reduced volume-regulated outwardly rectifying anion channel activity in ventricular myocyte of type 1 diabetic mice. *J. Physiol. Sci.* 59, 87–96. doi: 10.1007/s12576-008-0012-8
- Yang, X., and Qian, K. (2017). Protein O-GlcNAcylation: emerging mechanisms and functions. *Nat. Rev. Mol. Cell Biol.* 18, 452–465. doi: 10.1038/nrm.2017.22
- Yuzwa, S. A., and Vocadlo, D. J. (2014). O-GlcNAc and neurodegeneration: biochemical mechanisms and potential roles in Alzheimer's disease and beyond. *Chem. Soc. Rev.* 43, 6839–6858. doi: 10.1039/c4cs00038b
- Zachara, N., Akimoto, Y., and Hart, G. W. (2015). "The O-GlcNAc Modification," in *Essentials of Glycobiology*, eds A. Varki, R. D. Cummings, J. D. Esko, P. Stanley, G. W. Hart, M. Aebi, et al. (New York, NY: Cold Spring Harbor), 239–251.
- Zachara, N. E., and Hart, G. W. (2006). Cell signaling, the essential role of O-GlcNAc! *Biochim. Biophys. Acta* 1761, 599–617. doi: 10.1016/j.bbali.2006.04.007
- Zachara, N. E., O'Donnell, N., Cheung, W. D., Mercer, J. J., Marth, J. D., and Hart, G. W. (2004). Dynamic O-GlcNAc modification of nucleocytoplasmic proteins in response to stress. A survival response of mammalian cells. *J. Biol. Chem.* 279, 30133–30142. doi: 10.1074/jbc.M403773200
- Zeidan, Q., and Hart, G. W. (2010). The intersections between O-GlcNAcylation and phosphorylation: implications for multiple signaling pathways. *J. Cell Sci.* 123(Pt. 1), 13–22. doi: 10.1242/jcs.053678

Conflict of Interest: The authors declare that the research was conducted in the absence of any commercial or financial relationships that could be construed as a potential conflict of interest.

Copyright © 2020 Costa, Remigante, Civello, Bernardinelli, Szabó, Morabito, Marino, Sarikas, Patsch, Paulmichl, Janáky, Miseta, Nagy and Dossena. This is an open-access article distributed under the terms of the Creative Commons Attribution License (CC BY). The use, distribution or reproduction in other forums is permitted, provided the original author(s) and the copyright owner(s) are credited and that the original publication in this journal is cited, in accordance with accepted academic practice. No use, distribution or reproduction is permitted which does not comply with these terms.